AD 651 166

DISCLAIMER NOTICE

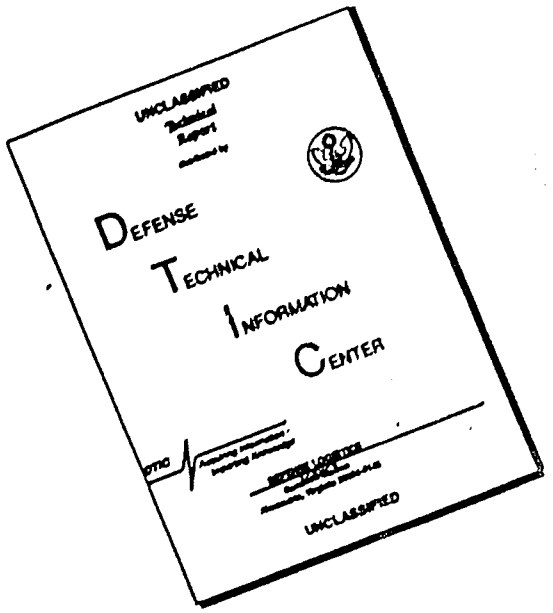

THIS DOCUMENT IS BEST QUALITY AVAILABLE. THE COPY FURNISHED TO DTIC CONTAINED A SIGNIFICANT NUMBER OF PAGES WHICH DO NOT REPRODUCE LEGIBLY.

FOREWORD

The work reported herein was sponsored by the United States Army Research Office, Durham, under Contract No. DA-31-124-ARO-D-246. The study presented herein was conducted by Mr. James L. Bishop in fulfilling the requirements for a thesis in his Master of Science program at The Ohio State University.

ABSTRACT

An experimental investigation was conducted on the use of corona wind in air as a means of triggering a fluid "flip-flow" amplifier element. The study centered on the ability to miniaturize the device previously shown possible in other work under the contract. Specific emphasis was also given to the nature of the connecting lines and plenum for the lateral control ports. The results of the investigation indicated that the miniaturized units required very small currents to flip the primary jet, and that the units were very sensitive to the configuration of the plenum and lateral lines.

TABLE OF CONTENTS

LIST OF ILLUSTRATIONS

LIST OF ILLUSTRATIONS (Continued)

LIST OF ILLUSTRATIONS (Continued)

LIST OF SYMBOLS

Symbol	
A	distance from positive corona wire to negative electrode plates
A_c	area control port outlet
A_n	area nozzle outlet
a	interaction width of flow channel
b	control port width
B	control port width at corona point
C	y-intercept current Re number plot
c	empirical constant
D	y-intercept power Re number plot
d	inlet nozzle width
e	base of natural logarithm
E	electrical field strength
F	body force
I	current
J	current density
K_o	positive ion mobility
L	length of flow channel wall
m	slope curren+ Re number plot
n	slope power Re number plot
p	power
p_s	static pressure
p_t	total pressure
Q	flow rate through nozzle

LIST OF SYMBOLS (Continued)

Symbol	
Q_c	flow rate through control nozzle
R	gas constant
Re	Reynolds number
s	distance from nozzle exit to splitter
V	channel velocity
V_c	control port velocity
V_n	mean nozzle velocity
V_o	maximum channel velocity for a given amplifier and flow
v	air velocity
v_i	velocity of ions in air
v_t	total ion velocity
w	nozzle and channel thickness
x	distance from corona point
ϵ	permittivitiy
μ	dynamic viscosity
ρ_c	gas density at control port
ρ_i	ion density
ρ_n	gas density at nozzle exit
σ_c	electrical conductivity
α	flow channel wall angle

I. INTRODUCTION

GENERAL OBJECTIVE

This investigation is designed to study the use of an electrical-to-fluidic transducer with no mechanical motions. Many electrical-to-fluidic transducers are available that require the electrical signal to produce a mechanical motion to control the fluidic device, but for direct conversion of an electrical-to-fluidic signal, the corona wind technique may offer a possible approach.

With the corona wind setup, a plenum chamber is attached to the large amplifier in an attempt to control the control port air flow and possibly result in a lower current for flipping.[1]

The large amplifier has been run successfully with open control ports.[1] The work done on this amplifier is the foundation of this investigation.

Miniaturizing is an important problem to overcome. Building a small amplifier to test the effects of miniaturization is the basic concern in this investigation. The addition of a plenum chamber is also possible for comparison with the large amplifier.

The small amplifier will also be designed with different geometries to test the effects the interaction width and channel angles will have on the flow.

HISTORY OF WALL ATTACHMENT ANALYSIS

It was noted by a Hungarian inventor, Henry Coanda, in 1933, that a thin jet sheet spewing into an unbounded region was deflected toward an adjacent wall. When the wall was reasonably close to the jet axis, the jet attached to and flowed along the wall[2] (see Fig. 1).

Other early notable work was done by McMahan in 1938, using a fluid dynamic control concept to control the flow of air through ducts or fan housings, and by Kline in 1958 with a wide-angle diffuser in demonstrating that the flow would separate from one wall and attach to the other or possibly flow in a stable position between the walls if they are too far apart.[2] This is the basic principle of the fluid amplifier in this investigation.

After the initial impetus was set forth in 1960 by the announcements from Harry Diamond Laboratory and Massachusetts Institute of Technology of their developments in fluid amplifier technology, several companies immediately entered into basic fluid amplifier research. The field has grown steadily since then with over 100 companies involved in actual production and research.[2]

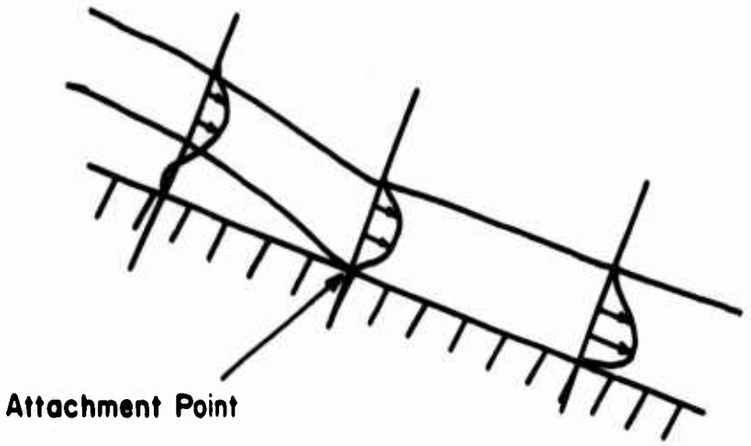

Fig. 1 - Velocity distribution along wall

Figure 2a shows a free jet emerging from a nozzle and dragging the ambient air along on both sides. When a wall is brought near the free jet, Fig. 2b, the flow will deflect toward the wall because of the lower pressure on that side of the jet. The lower pressure is a result of cutting off the entrainment flow on the wall side of the jet. As the jet deflects, the entrainment is reduced even further and a greater deflection occurs. With the proper geometry the flow may deflect far enough to attach itself to the adjacent wall, Fig. 3a. When attachment does occur, a closed region is formed with the jet and walls as boundaries and is commonly called a separation bubble. With low pressure existing in the closed region and ambient pressure on the other side of the jet, the pressure gradient thus holds the jet against the wall indefinitely.

Now to put this principle of wall attachment to use in a fluid amplifier, two control ports are added, Fig. 3b. When air is forced through the control ports into the bubble region, the increase in pressure, if sufficient, detaches the jet from the wall and switches it to the other side where it is in a stable position until the process is reversed, even though the air may stop flowing in the opposite control port. By regulating the flow in the control ports, the simple wall attachment device now becomes a basic fluid amplifier.

To point out a few principles of attachment, assume the flow attaches itself to the left wall of the amplifier, Fig. 4. Air is continuously flowing through the control port to replenish entrained air and there is also a backflow of air through the right channel. When the main flow is increased, the reattachment point moves downstream and more air is entrained from the higher mass flow of air. Since the jet requires more air for entrainment in the bubble than is available, a lower pressure results. With a larger pressure gradient across the jet, the flow is now harder to switch. Just the opposite effect occurs when the main flow is decreased. A typical fluid amplifier geometry is shown in Fig. 5.

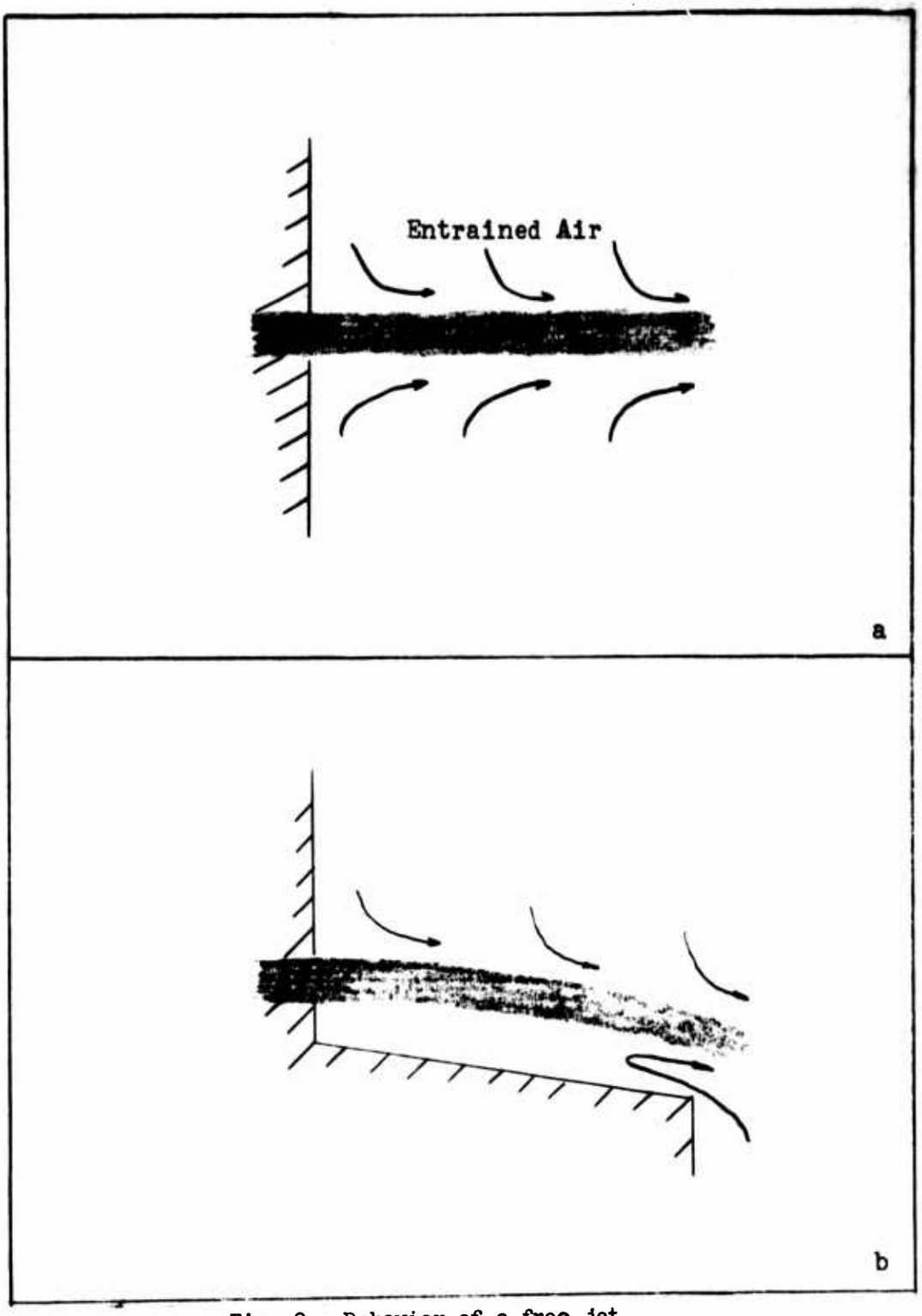

Fig. 2 - Behavior of a free jet

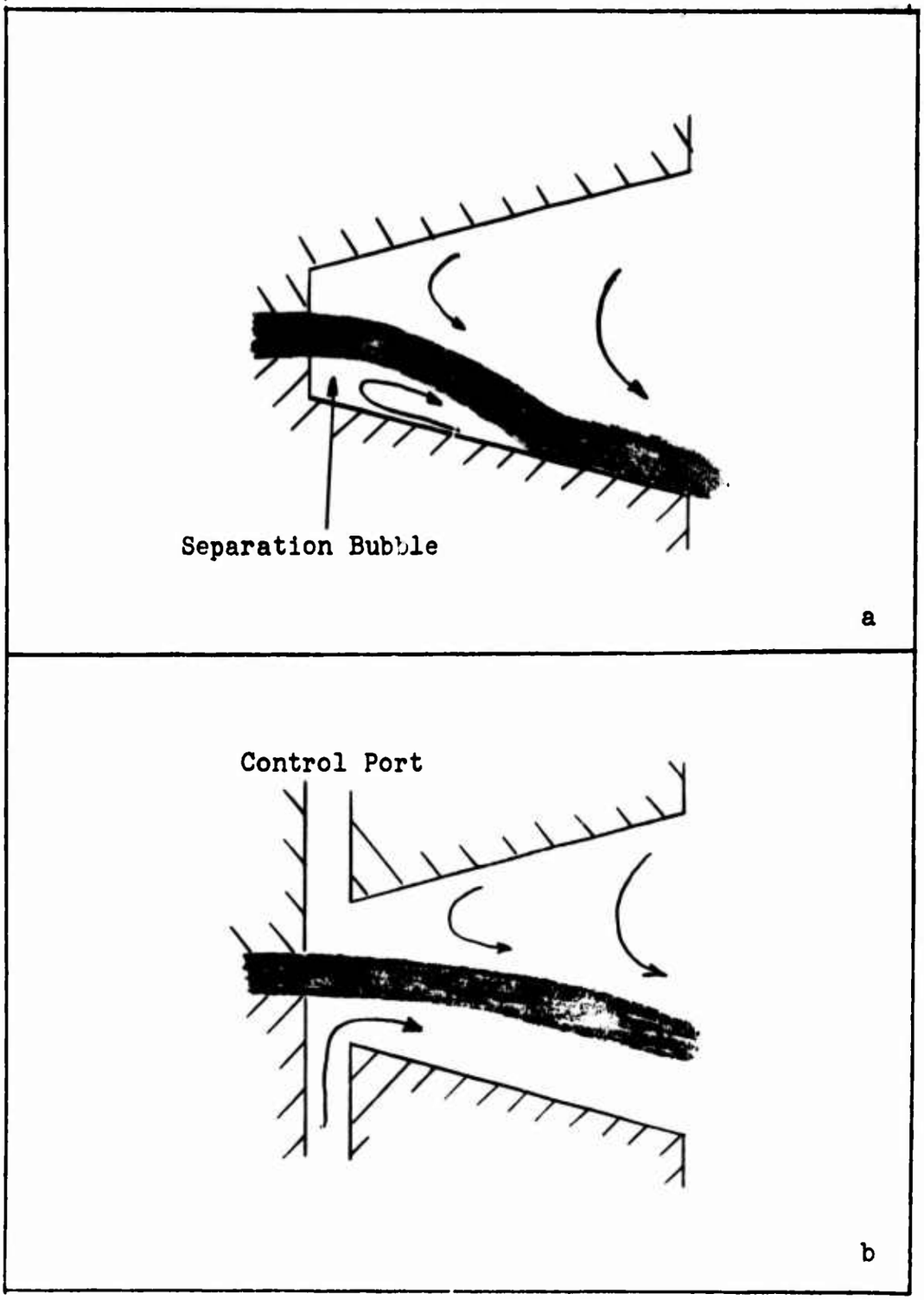

Fig. 3 - Behavior of a free jet

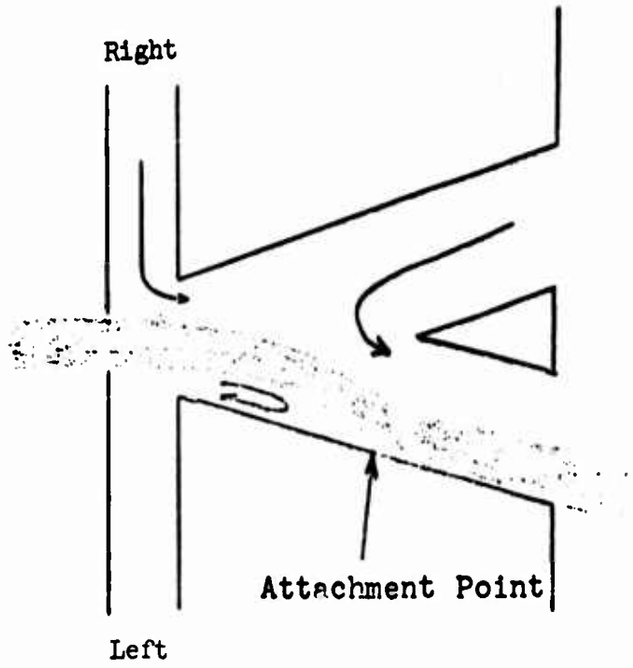

Fig. 4 - Attachment in a fluid amplifier

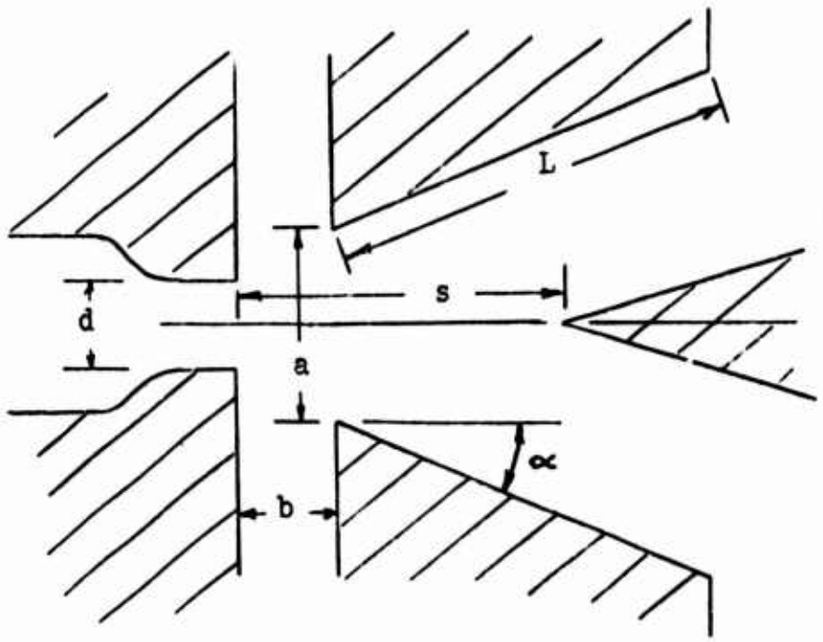

Fig. 5 - Typical fluid amplifier geometry

ELECTROSTATIC FORCES

An electric field can be used to move charged particles and can also affect neutral particles as well. Small body forces resulting from the movement of the uncharged particles may be sufficient to affect the flow attachment.

One method of moving the air is the electric wind phenomenon shown in Fig. 6. At the point of a highly charged needle a very intense electric field exists that is known as a corona discharge. The air around this point is highly ionized from the collision of electrons with neutral particles. The ions created in the region are always seeking a lower potential and, therefore, move away from the needle to the negative electrode where the field strength is lower.[3,4,5] Appendix I gives a detailed analysis of the corona discharge and the resulting corona wind.

The high acceleration of ions away from the corona point causes a negative pressure gradient from the control port inlet to the corona point causing air to flow in the port to the corona point where it replenishes the air that is flowing toward the negative plates. During this process there is a momentum exchange between the ions and neutral particles downstream of the point which causes a local mass motion or wind on the macroscopic level.

The operation of the electric wind phenomenon is limited to the power requirements needed to produce sufficient wind and the potential that can be applied before breakdown (sparking) occurs. This mass motion should be sufficient to flip a stream of air in a fluid amplifier if the proper conditions exist.

II. EXPERIMENTAL APPROACH

EXPERIMENTAL APPARATUS

To study the general objectives of this investigation, a fluid amplifier constructed of Plexiglas was used in the experimental setup shown in Fig. 7. The details of this apparatus are follows.

Air Inlet Nozzle

For each amplifier the air inlet is a rectangular 0.40 x 0.25-inch hole with two wire screens placed across the channel to smooth out the incoming air flow. The nozzle narrows to a 0.20 x 0.25-inch outlet where the flow is approximately one-dimensional.

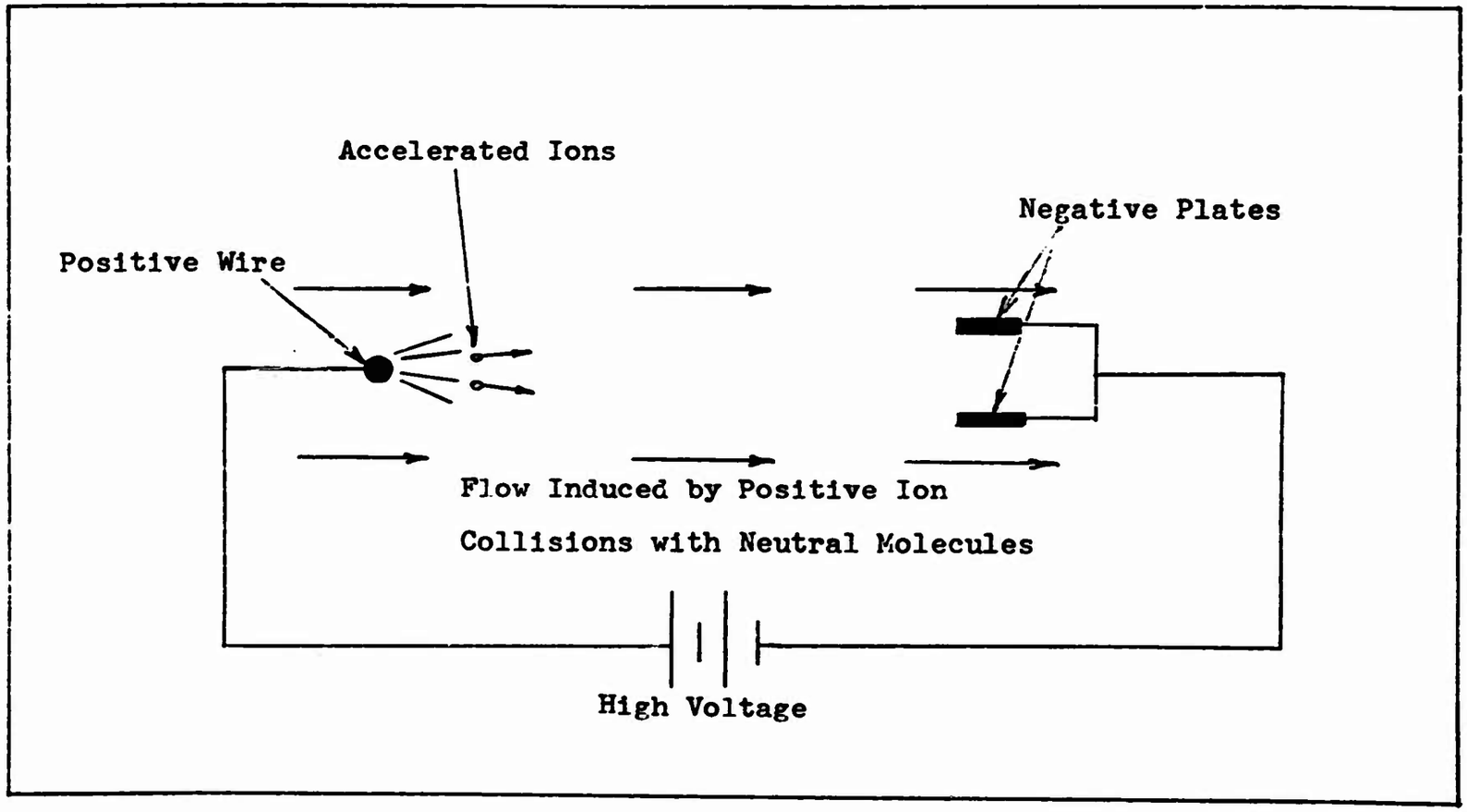

Fig. 6 - Corona wind from a charged wire

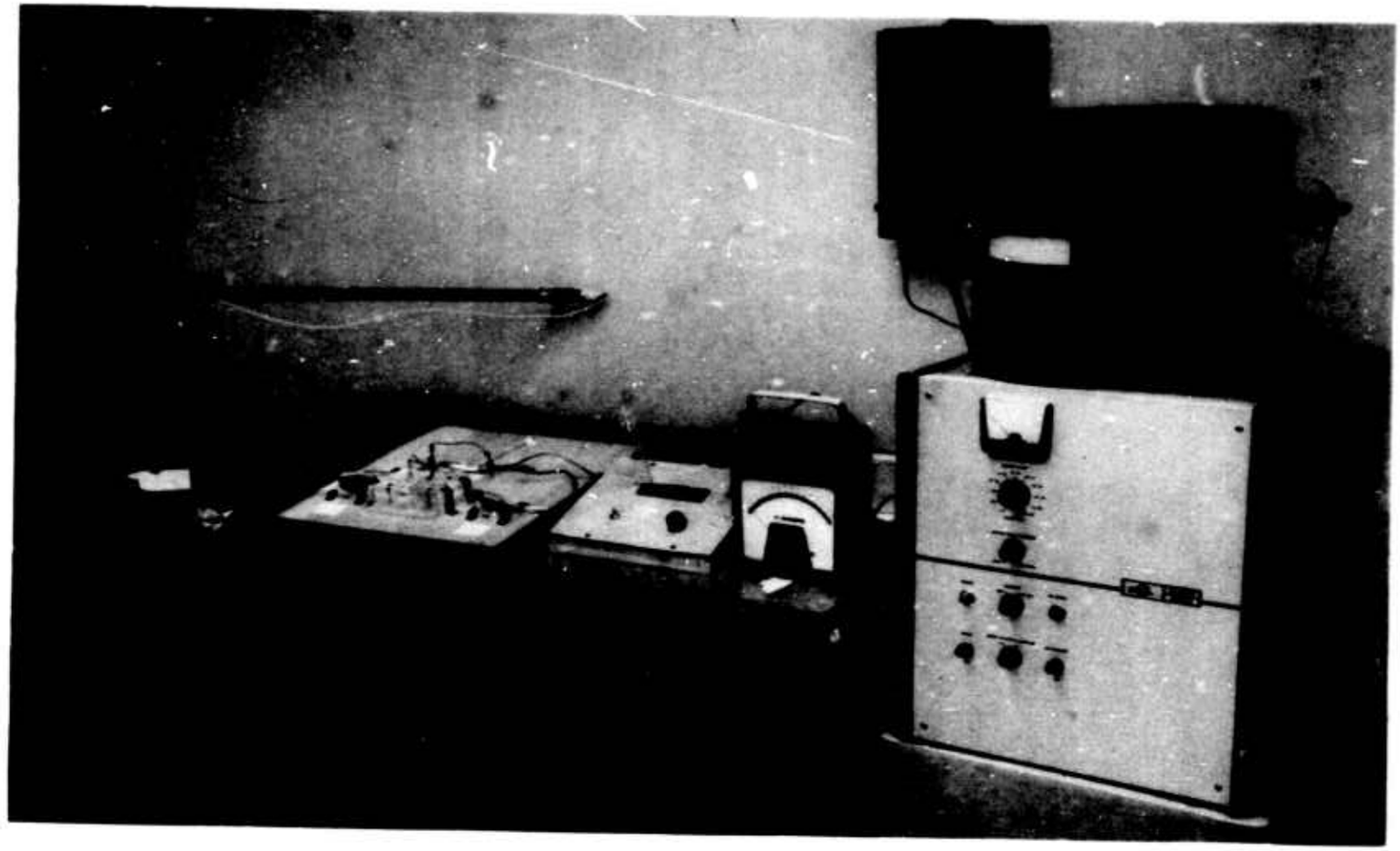

Fig. 7 - Over-all view of test setup. Inclined manometer, left; switch and microammeter, center; Sorensen high voltage power supply and electrostatic voltmeter, right

Flow Channel

Three different configurations are used for the fluid amplifier (see Figs. 8-13), each one varying in interaction width or diverging angle. The large amplifier previously tested[1] is shown in Figs. 14 and 15. Each configuration is characterized by a number, i.e., Amplifier No. 1, No. 2, or No. 3. A splitter is inserted in the channel to give a better distinction of wall attachment and is positioned one inch downstream of the nozzle outlet. The distance of the flow channel from the nozzle outlet, b, is held constant at 0.15 inch for each amplifier.

Control Port

For each amplifier the control ports are identical. The outlet is 0.15 inch wide, which corresponds to the distance b from the nozzle to the flow channel. The control port inlet is one inch wide and tapers at a 30° angle to a 0.40-inch width (see Fig. 9).

Electrode Configuration

The positive electrode of 0.008-inch steel wire is used for all tests. Several sewing needles were tried, but their tips quickly burned out and inconsistent results were obtained. The positive electrode is centered horizontally and vertically in the control port and its distance from the negative electrode, A, can be varied from one-half inch to outside the port if needed. The negative electrodes consist of two plates, 1/4 x 3/16 x 1/32 inches, mounted on each side of the control port as shown in Figs. 8 and 9.

Power Supply

A Sorensen high-voltage power supply is used to supply the voltage to the positive corona wire. The output voltage is ripple free within the measurements of a cathode-ray oscilloscope, about one-half of one per cent. One problem is encountered with the voltage scale selector; with each jump in voltage on the large scale (3000 volts) the current sometimes changes for the same voltage from the sudden increase in voltage. By waiting a short time or adjusting the small-scale knob, the current readjusts to the previous value. This is only true at high voltages when the current is more sensitive to voltage changes.

Overall Test Setup

The overall test setup includes a Sorensen high-voltage power supply, an electrostatic voltmeter, a microammeter and an inclined manometer that are described in Appendix II. There is also a control console and mounting board shown in the overall test view (Fig. 7).

The amplifier is held in position by four brackets attached to the board. Likewise, each corona wire mount is positioned by four brackets, but the mount is capable of sliding left or right to position the corona point.

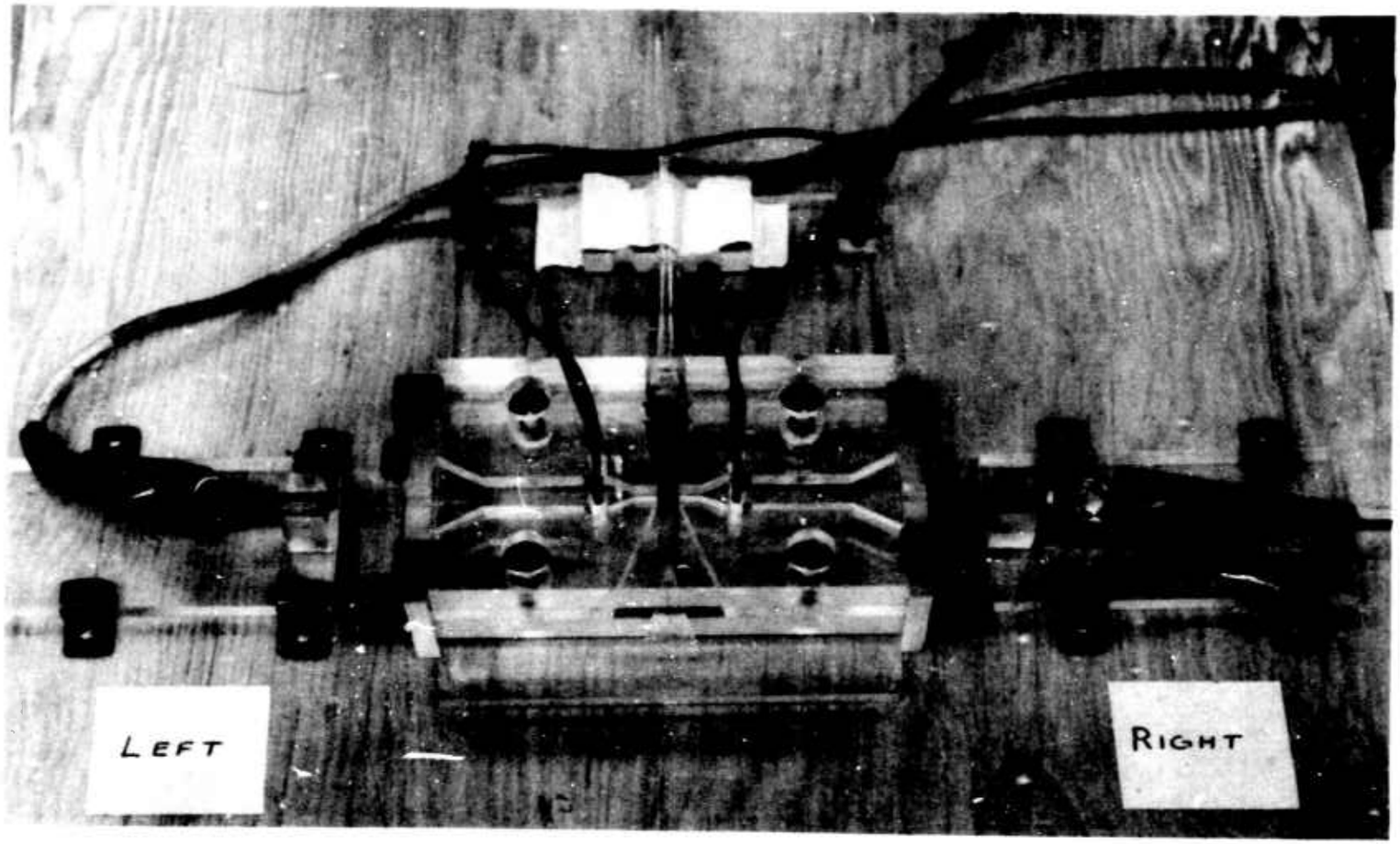

Fig. 8 - Close-up view of Amplifier No. 1 and postive electrodes (side plates are mounted for hoses)

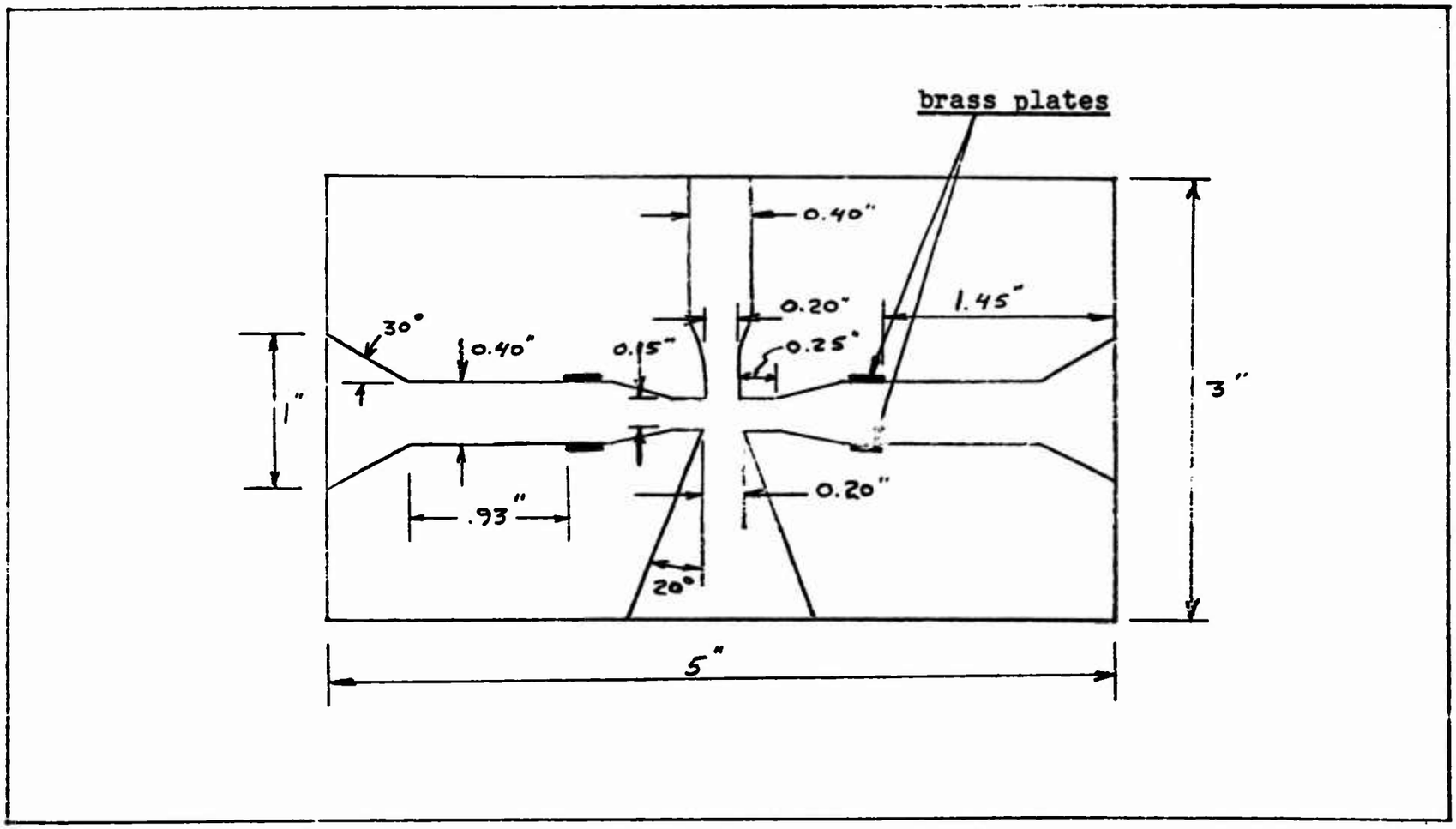

Fig. 9 - Diagram of Amplifier No. 1

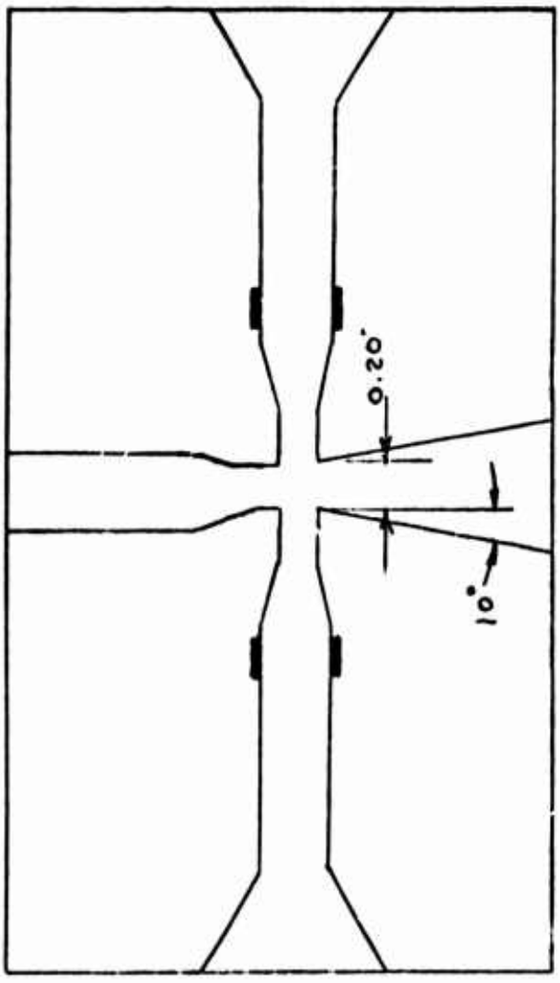

Fig. 10 - Diagram of Amplifier No. 2

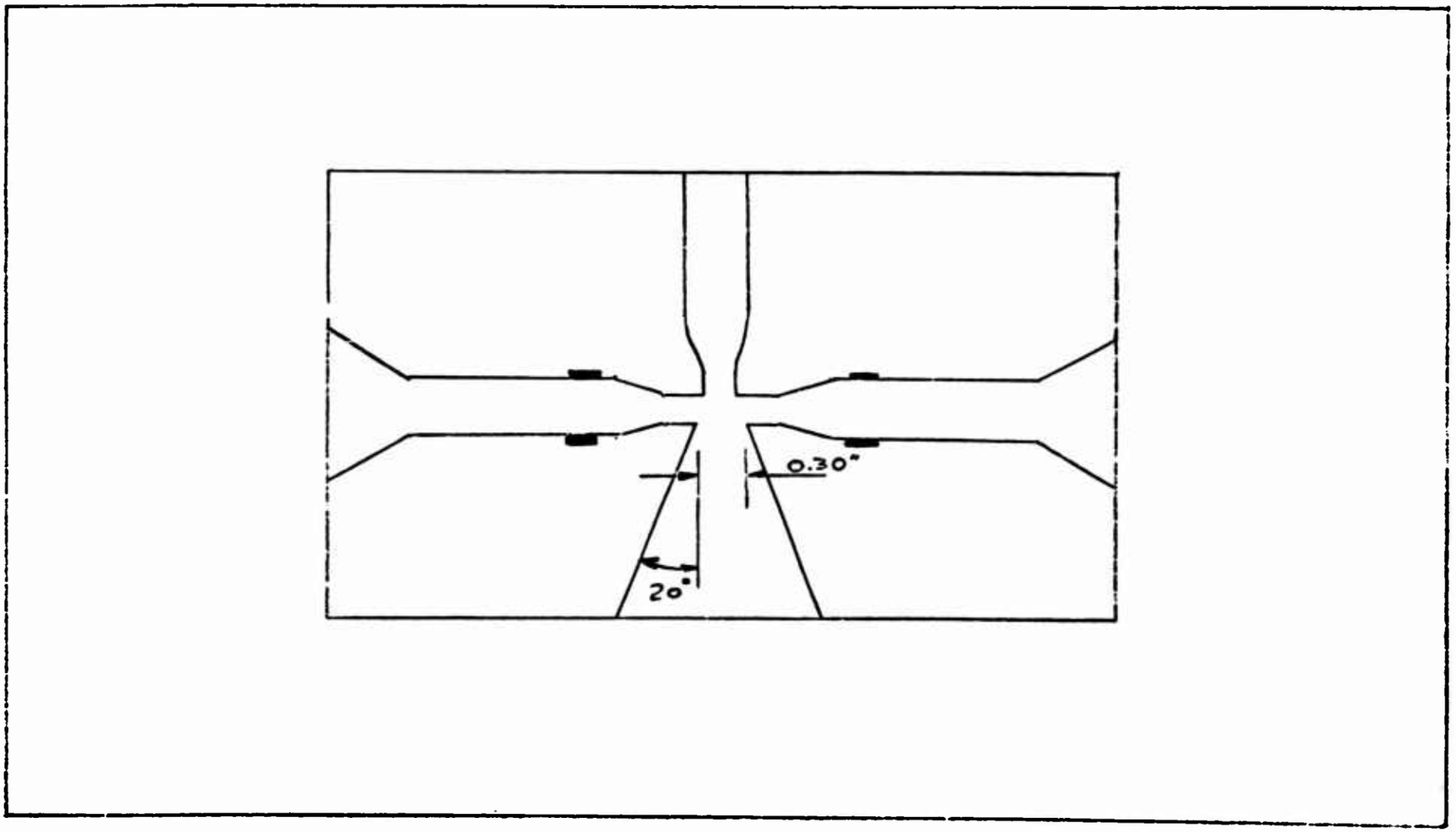

Fig. 11 - Diagram of Amplifier No. 3

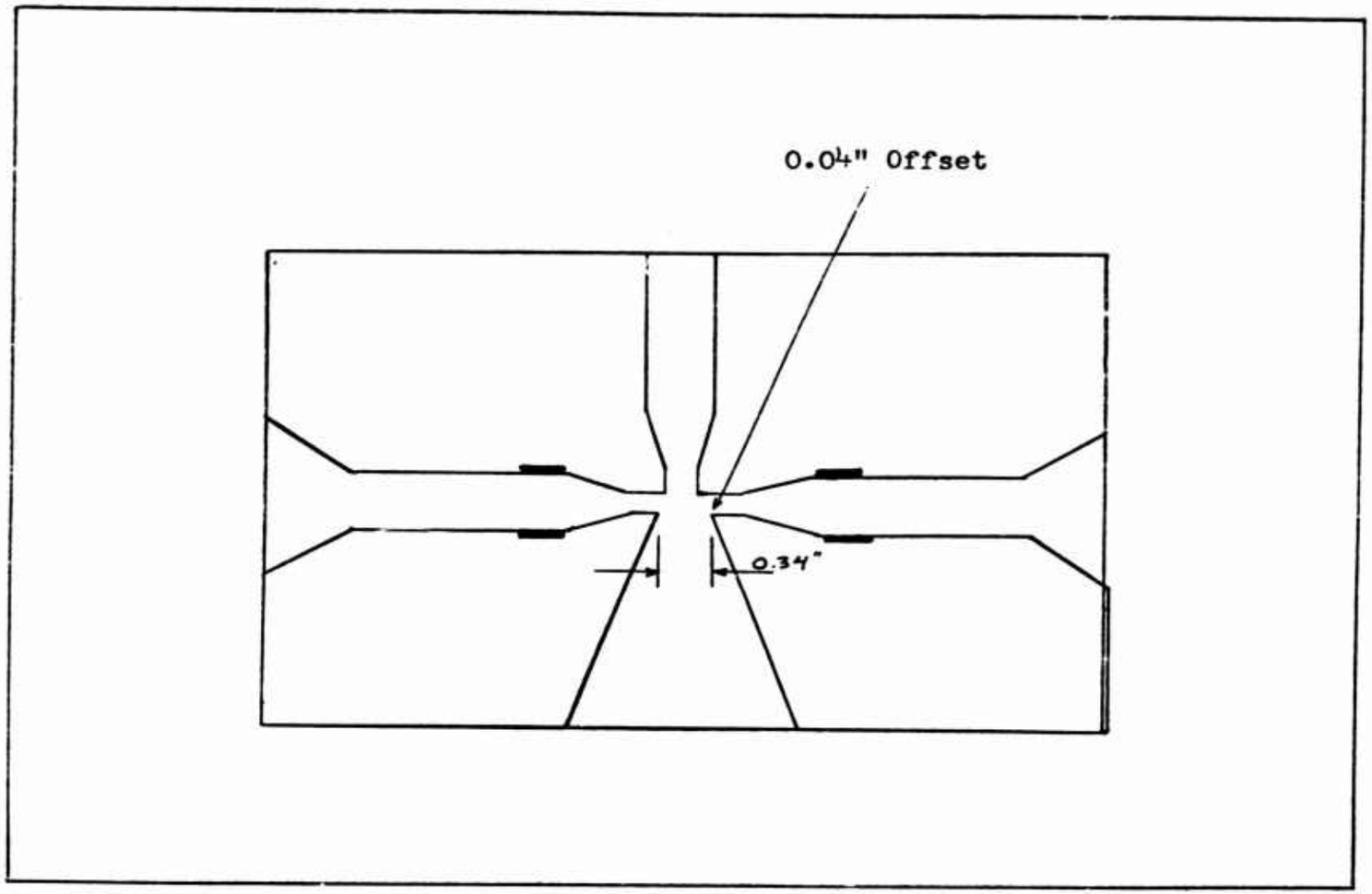

Fig. 12 - Amplifier No. 3 with skewed right channel

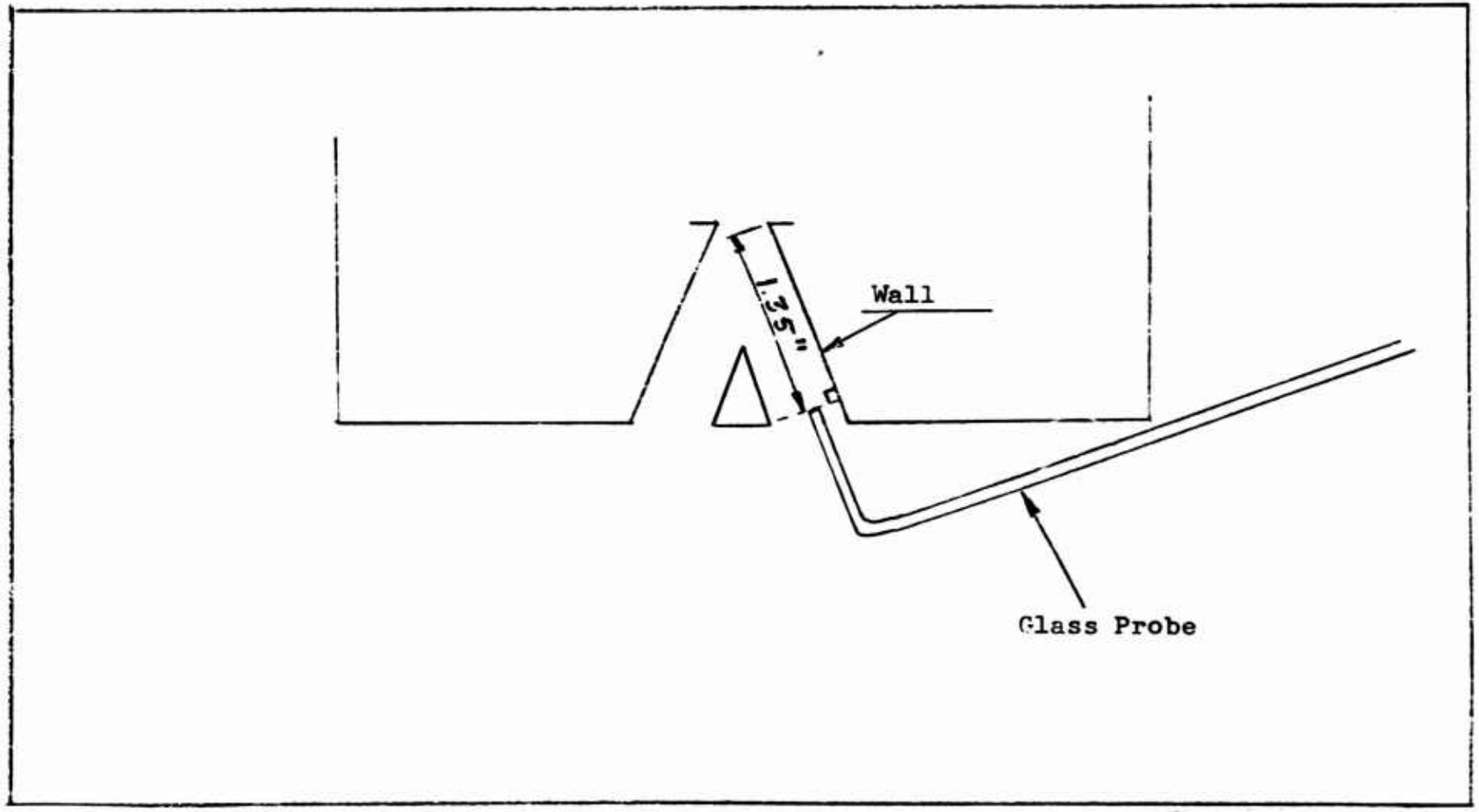

Fig. 13 - Measuring position for total pressure in channel

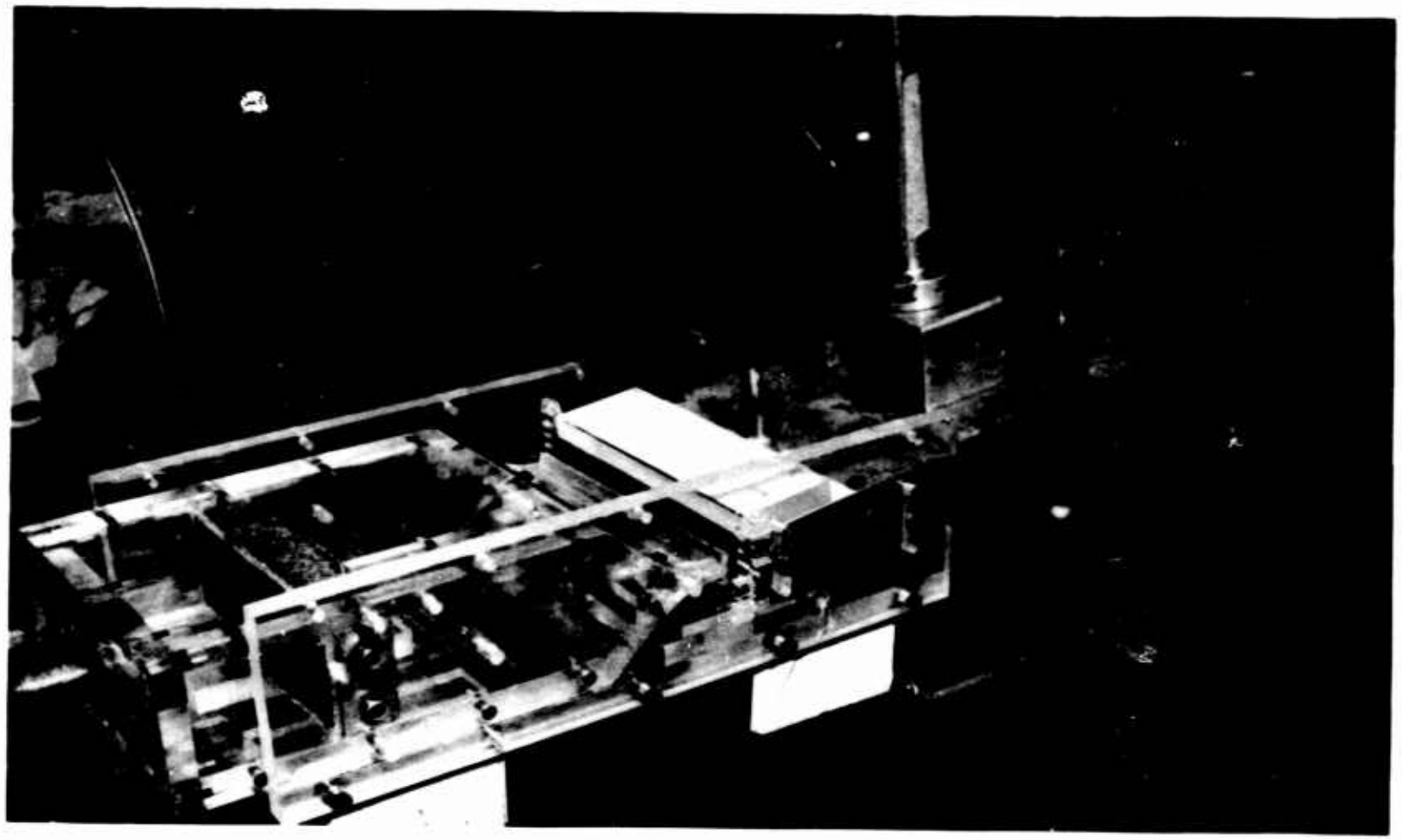

Fig. 14 - Close-up of large amplifier without control nozzles

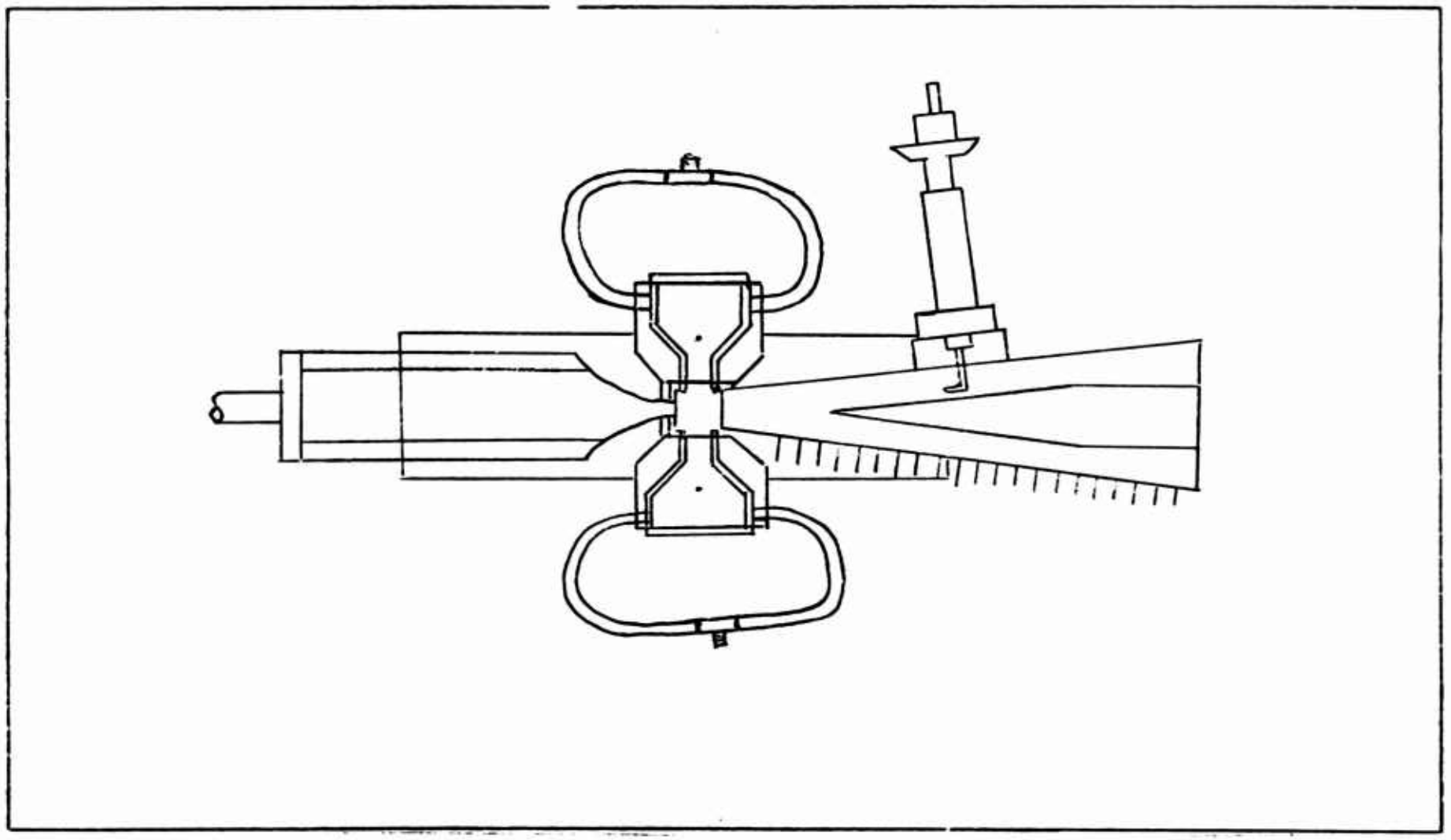

Fig. 15 - Diagram of large amplifier showing control nozzles and hoses

The air supply is brought to the amplifier by a 3/8 O. D. Tygon tubing and held in place by a support block. The air flow can be regulated by the two valves shown in Fig. 7. Figure 8 and 16 show photographs of the experimental arrangement.

The electrical connection on the left and right corona wires is made through a screw to give a positive connection to the small wire. The two high-voltage wires are connected to a single-pole, double-throw switch, mounted on the control console, that in turn is connected to the power supply. There are two other switches on the control panel, one for cutting the ammeter in and out of the circuit; the other to ground the negative plates past the ammeter. The ground wires extend from the top of the amplifier and connect to one common wire so either set of plates is grounded at all times. The electrostatic voltmeter is connected between the voltage source and ground.

Flow Measurement

The total pressure at the nozzle outlet was measured with the total pressure probe in the micrometer traverse. The pressure was practically constant across the outlet, thus indicating an approximate constant velocity profile. The velocity measured in the center was used for Reynolds number and flow-rate calculations.

A plot of the Reynolds number for various pressure readings is shown in Fig. 17.

Large Amplifier

The large amplifier used for initial plenum chamber tests was extensively tested in a previous investigation.[8] The amplifier as shown in Fig. 15 was built to incorporate four hoses attached from the control ports to the plenum chamber.

EXPERIMENTAL PROCEDURE

For the large amplifier a series of tests were run with various stages of the plenum chamber attached, i.e., hoses, hoses hooked together (see Figs 18 and 19), and hoses hooked to plenum chamber. These tests were to determine if the large amplifier can be made bistable when the control ports were attached to a plenum chamber. Each test consists of running at a certain nozzle Reynolds number and attaching the flow to the top plate then increasing the voltage until the current is sufficient to flip the flow. The same procedure is repeated in the other direction.

The small amplifier was built with interchangeable flow channels to achieve different geometric configurations for testing. Five tests were run with one of the three configurations designated Amplifier No. 1, No. 2, or No. 3.

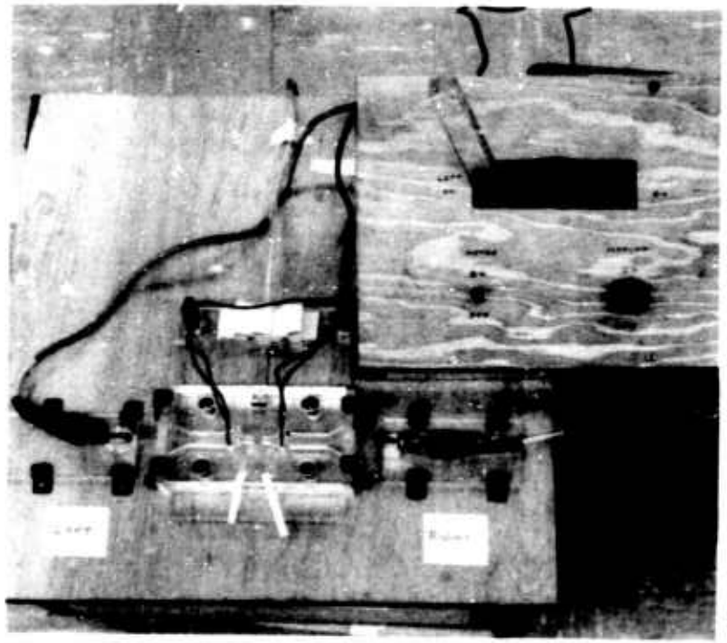

Left electrode on

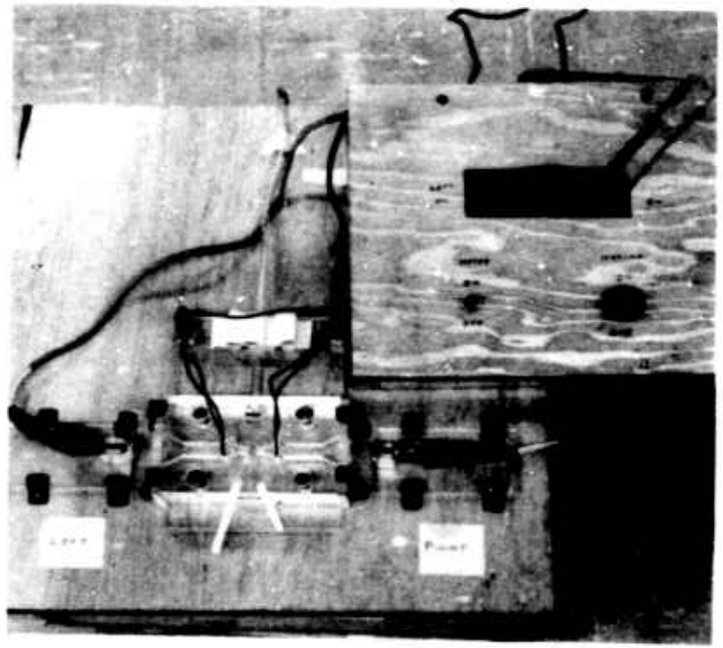

Right electrode on

Fig. 16 - Switching principle for amplifier

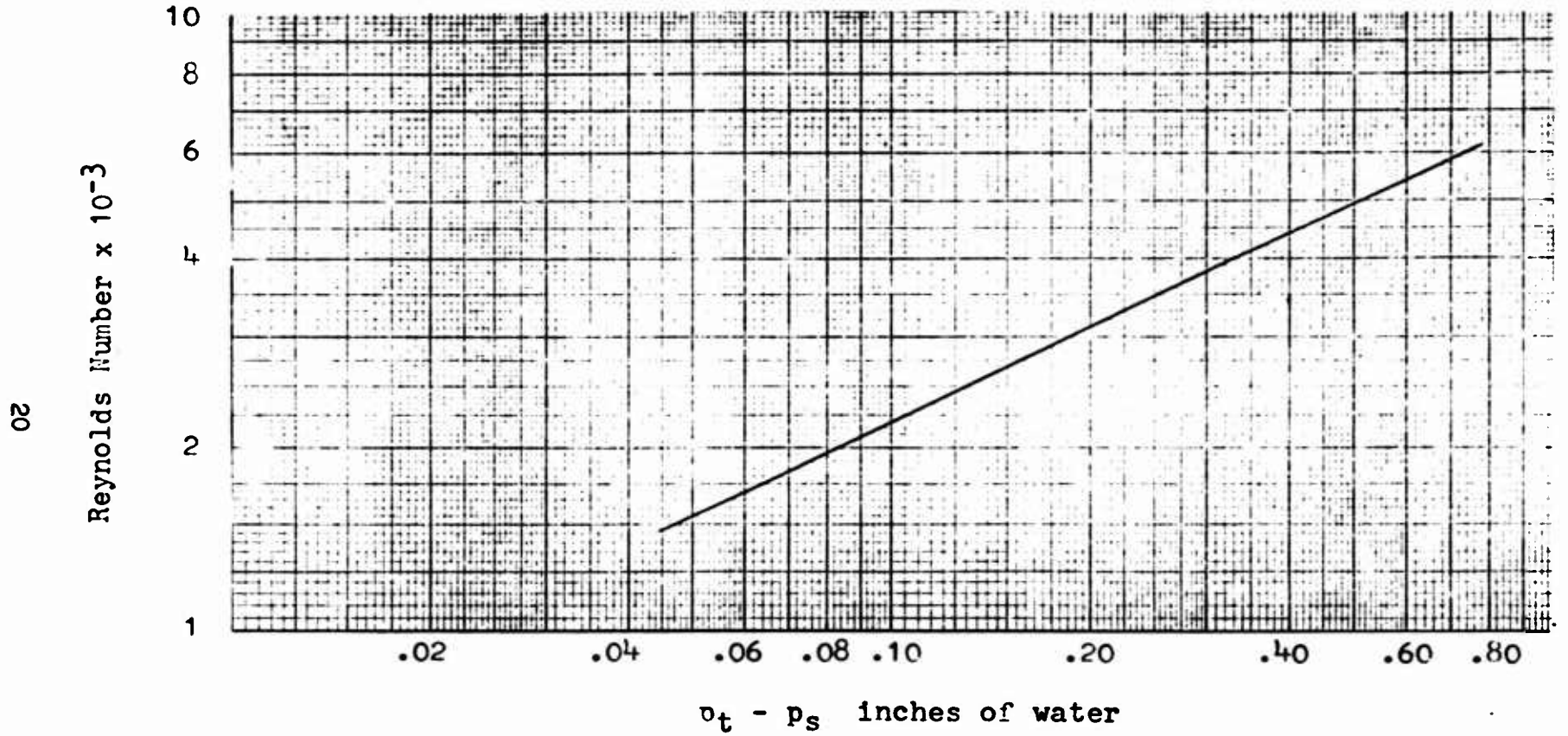

Fig. 17 - Nozzle Reynolds number for various total pressures

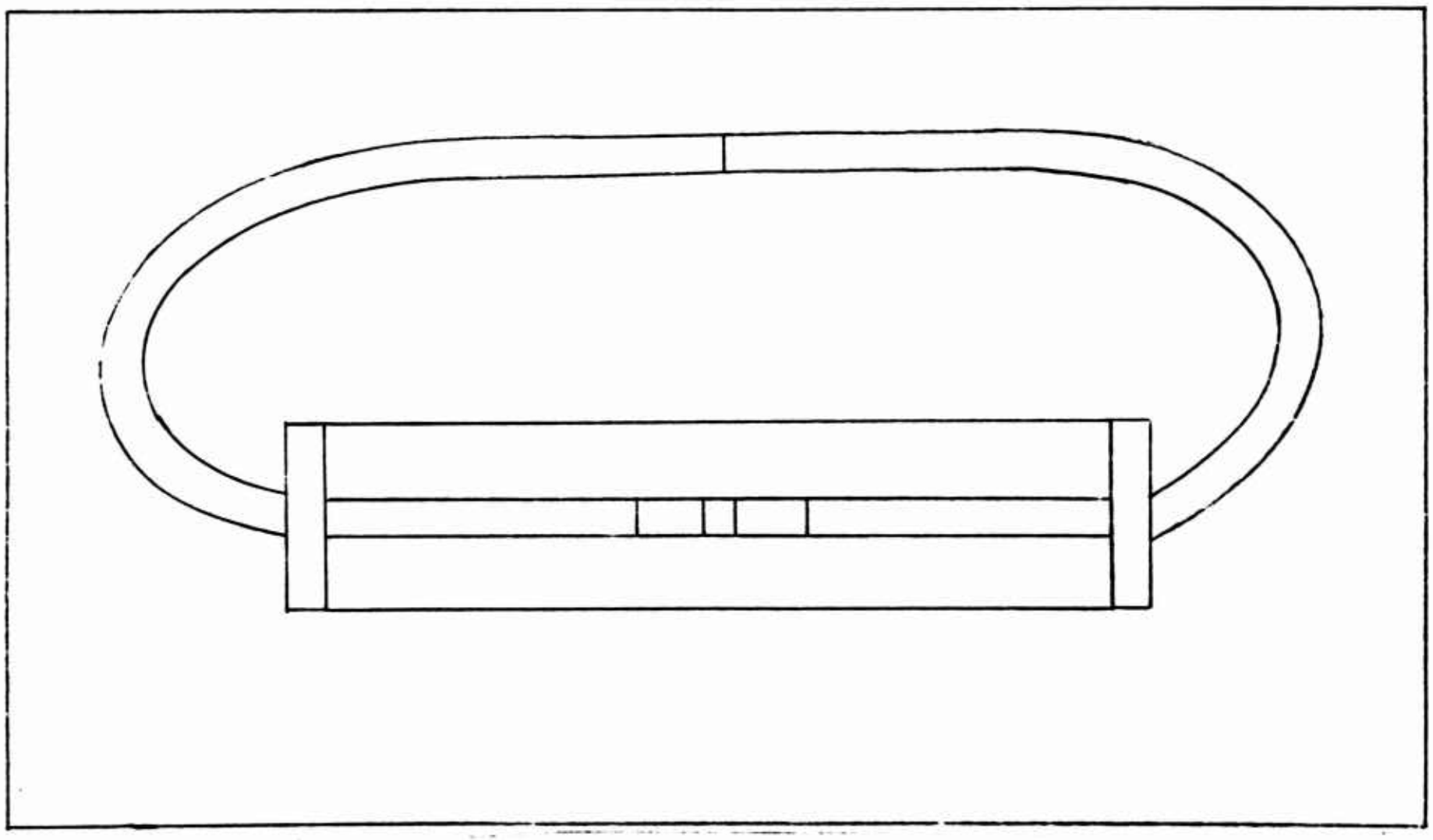

Fig. 18 - Diagram of amplifier with hoses directly connected

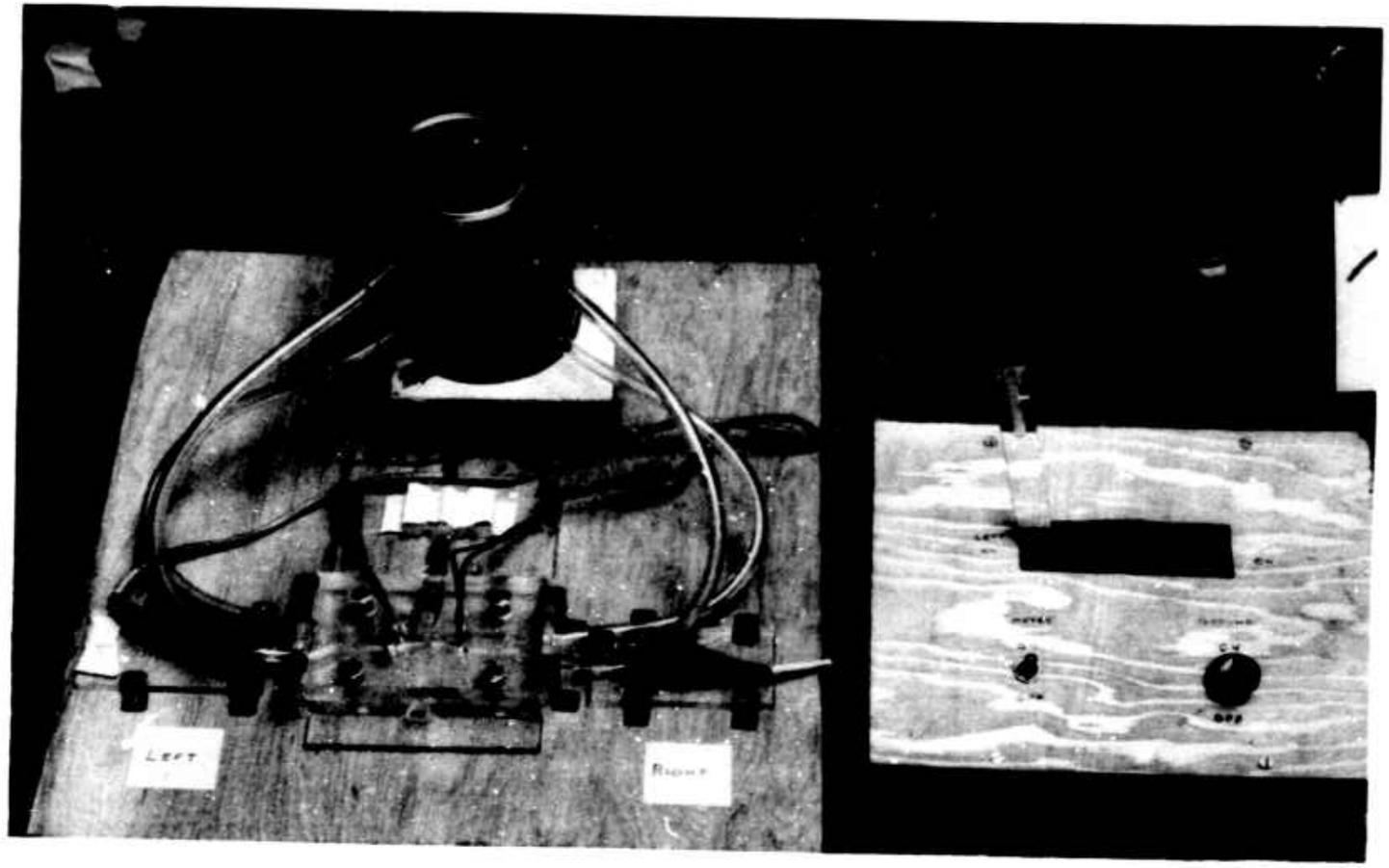

Fig. 19 - Test setup with plenum chamber

The procedure and purpose of each test was follows:

Test 1 - Using Amplifier No. 1, record the current and voltage required to flip the flow from right to left and left to right, calculate the power required, and measure the pressure distribution at the channel outlet for various Reynolds numbers. The purpose of this test is to record the performance of Amplifier No. 1 for comparison with other tests (see Figs. 20-26).

Test 2 - The same procedure and purpose used in test 1 is followed here only for amplifier No. 2 (see Figs. 27-34).

Test 3 - The same procedure is used only the purpose in this test is to also compare the effects of a skewed channel on the current and power requirement for Amplifier No. 3 (see Figs. 35-42).

Test 4 - Amplifier No. 1 is used for testing plenum chamber effects on performance. Separate runs are made to record current, voltages, and pressures with different parts connected to the control ports (see Table I and Figs. 43 and 44).

Test 5 - This test is an experimental study of the corona wind to determine velocities in the control port. For currents of 1.00, 1.25 and 1.50 microampere, the total and static pressure is measured along the control port (see Figs. 45-53).

Figure 16 shows the switching procedure used for all tests. Consider the flow attached to the left wall, to flip it to the right the switch is thrown to the "left on" position. This puts the corona discharge on the left side and creates a wind blowing from left to right. When the wind is strong enough, the flow flips to the right. The reversed procedure is used to flip from right to left.

Therefore, "right on" indicates flipping from right to left, "left on" from left to right. Any data marked as right means the right electrode is on and the flow is flipping from right to left.

Figure 20

Description of Test 1

Positive Electrode	0.008-inch steel wire
Negative Electrode	1/4 x 3/16 x 1/32-inch brass plates
Distance between Electrodes, A	3/4 and 1 inch
Amplifier	No. 1
Flow Channel Angle	20°
Interaction Width	0.20 inch
Splitter Position, s	1.0 inch
Current	0-3 microampere
Voltage	0-23 kilovolts
Reynolds Number	1750-3000

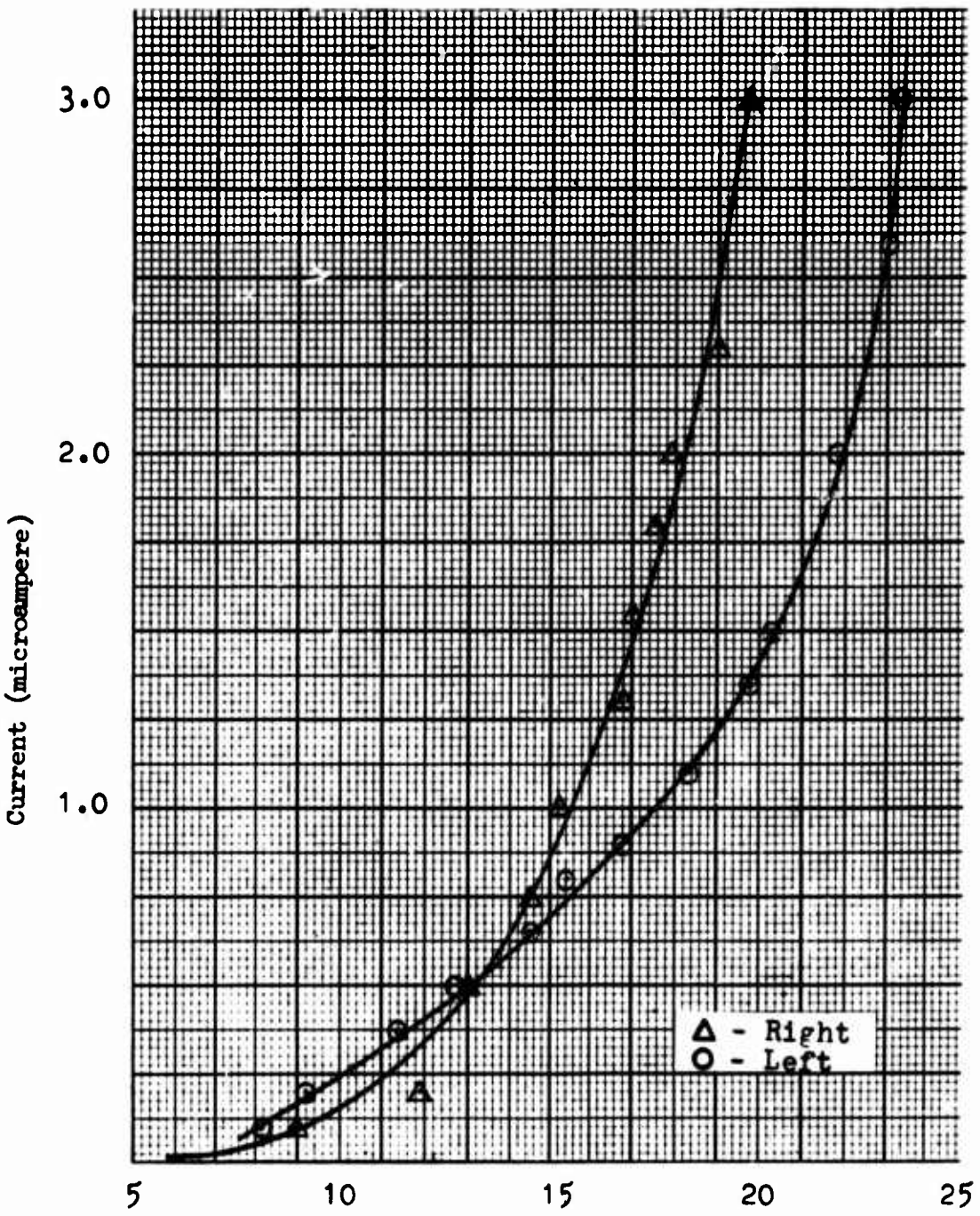

Fig. 21 - Current-voltage relation. A = 1 inch

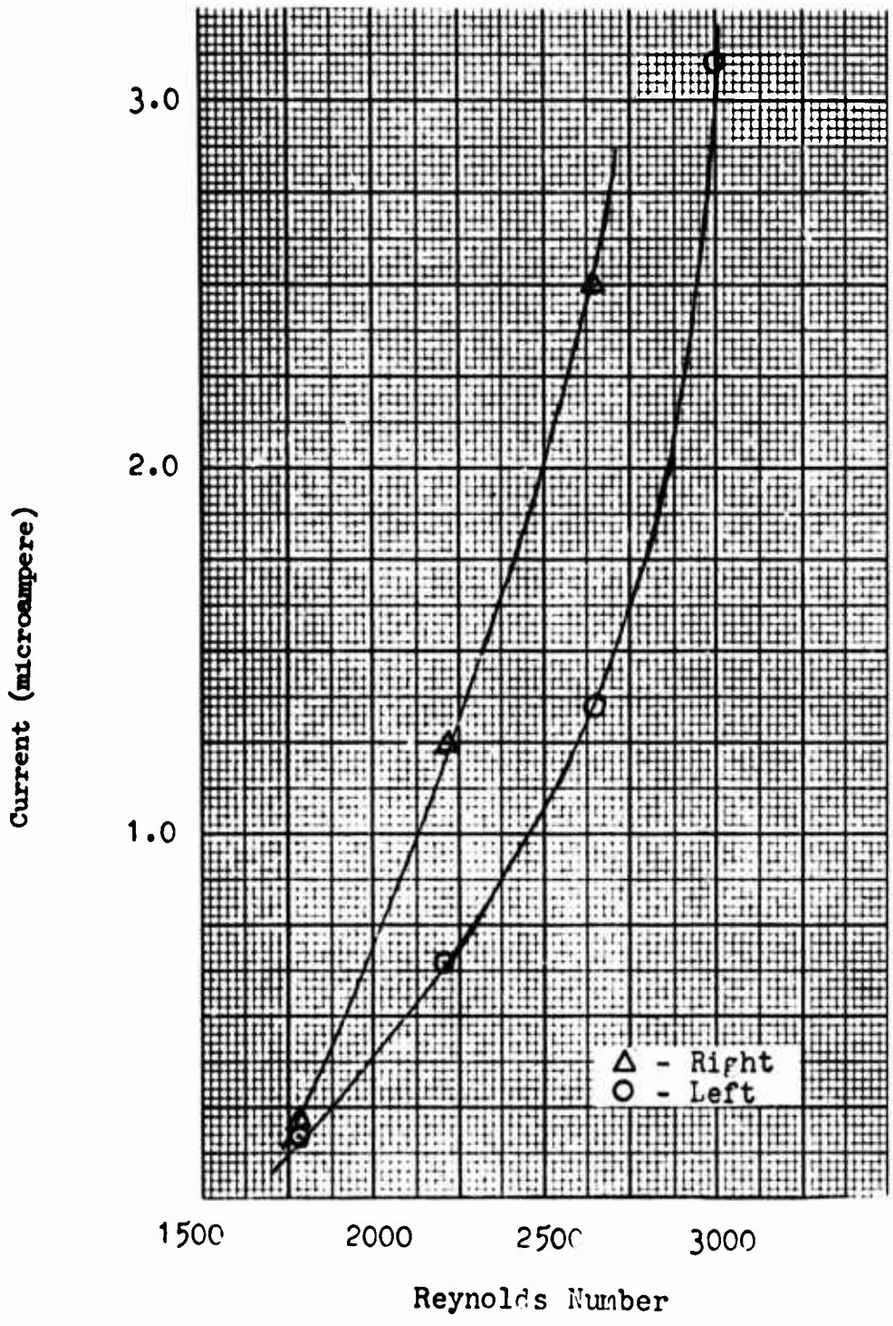

Fig. 22 - Current required to flip flow for various Reynolds numbers. A = 1 inch

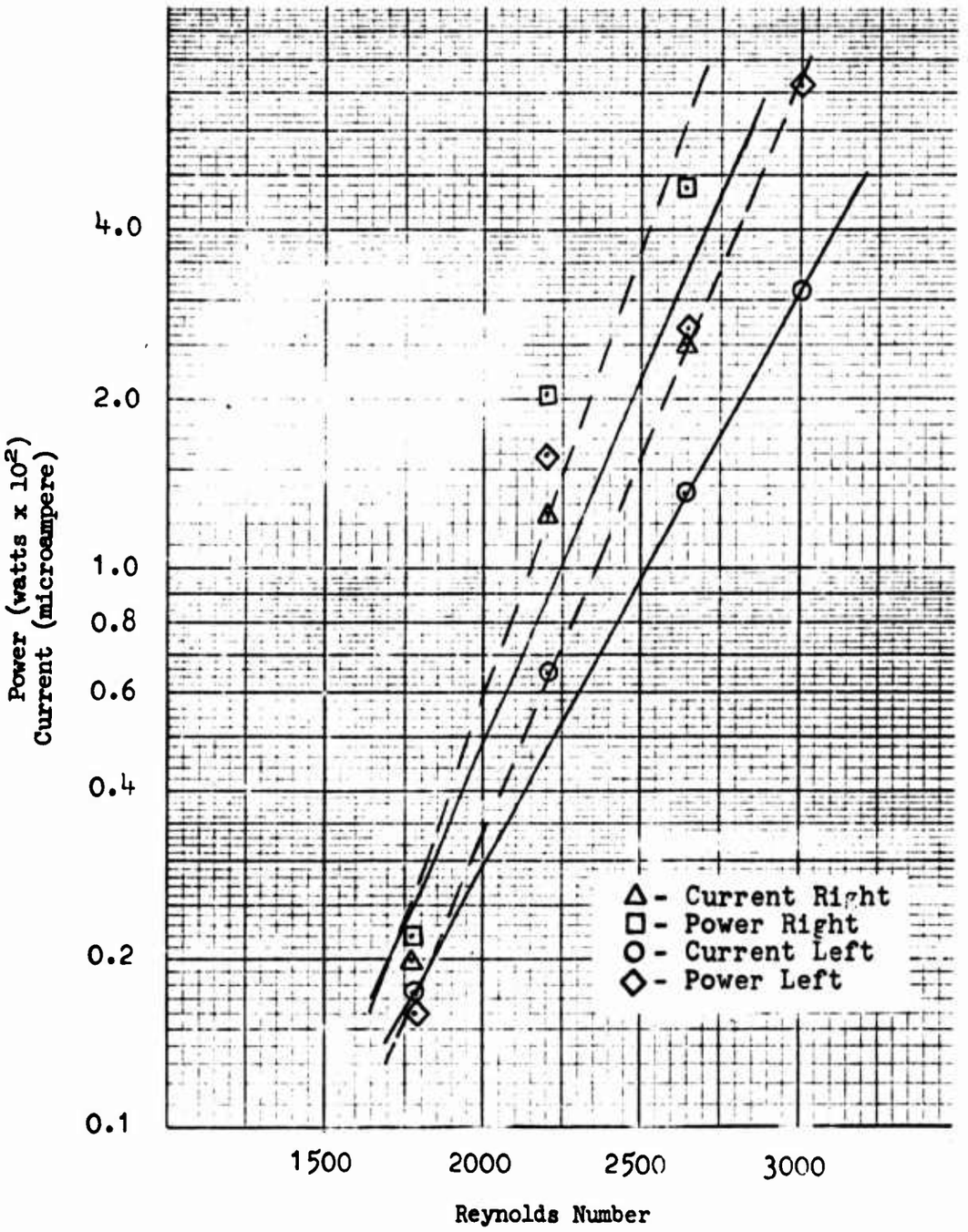

Fig. 23 - Current and power required to flip flow both directions. A = 1 inch

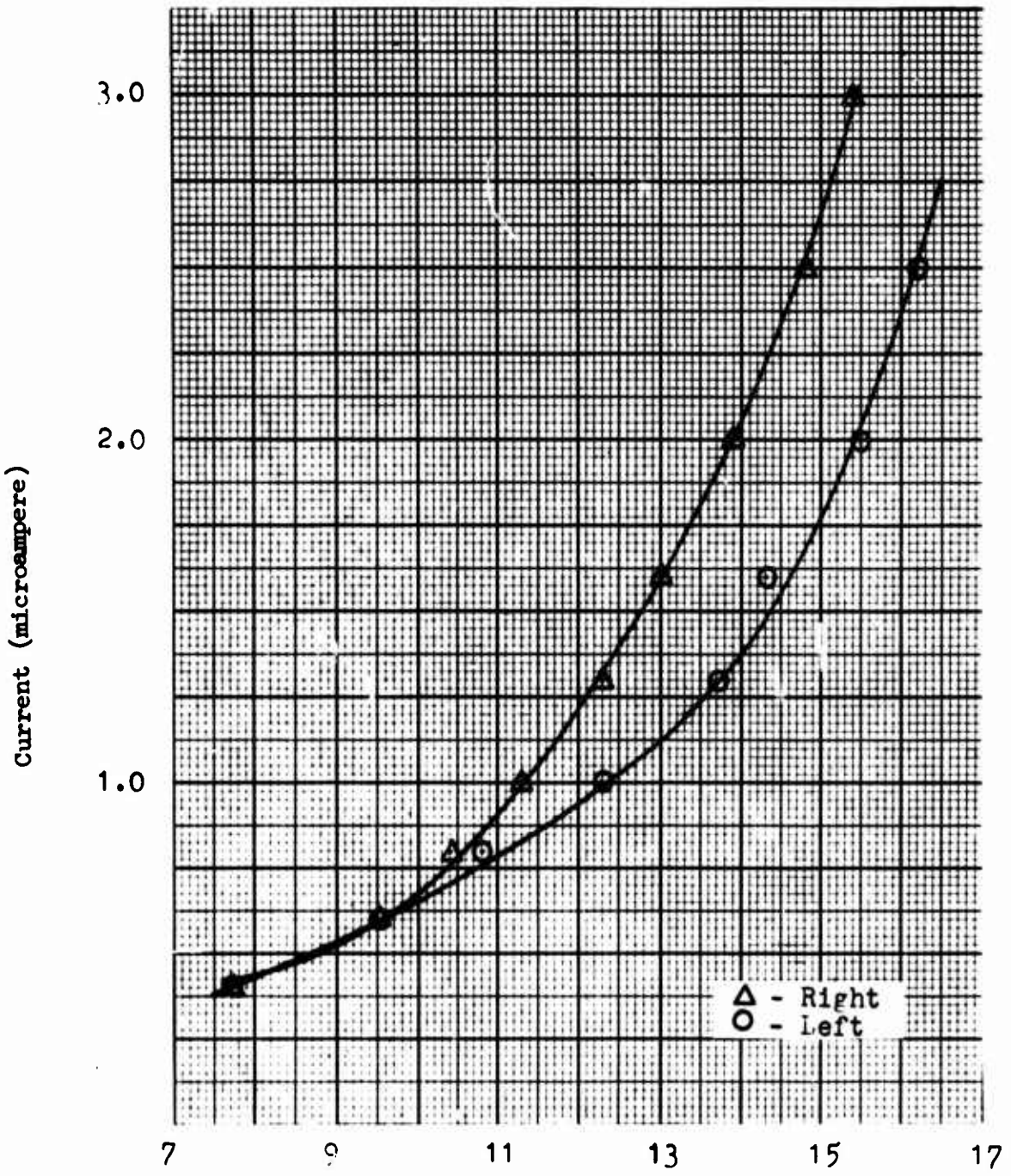

Fig. 24 - Current-voltage relation. A = 3/4 inch

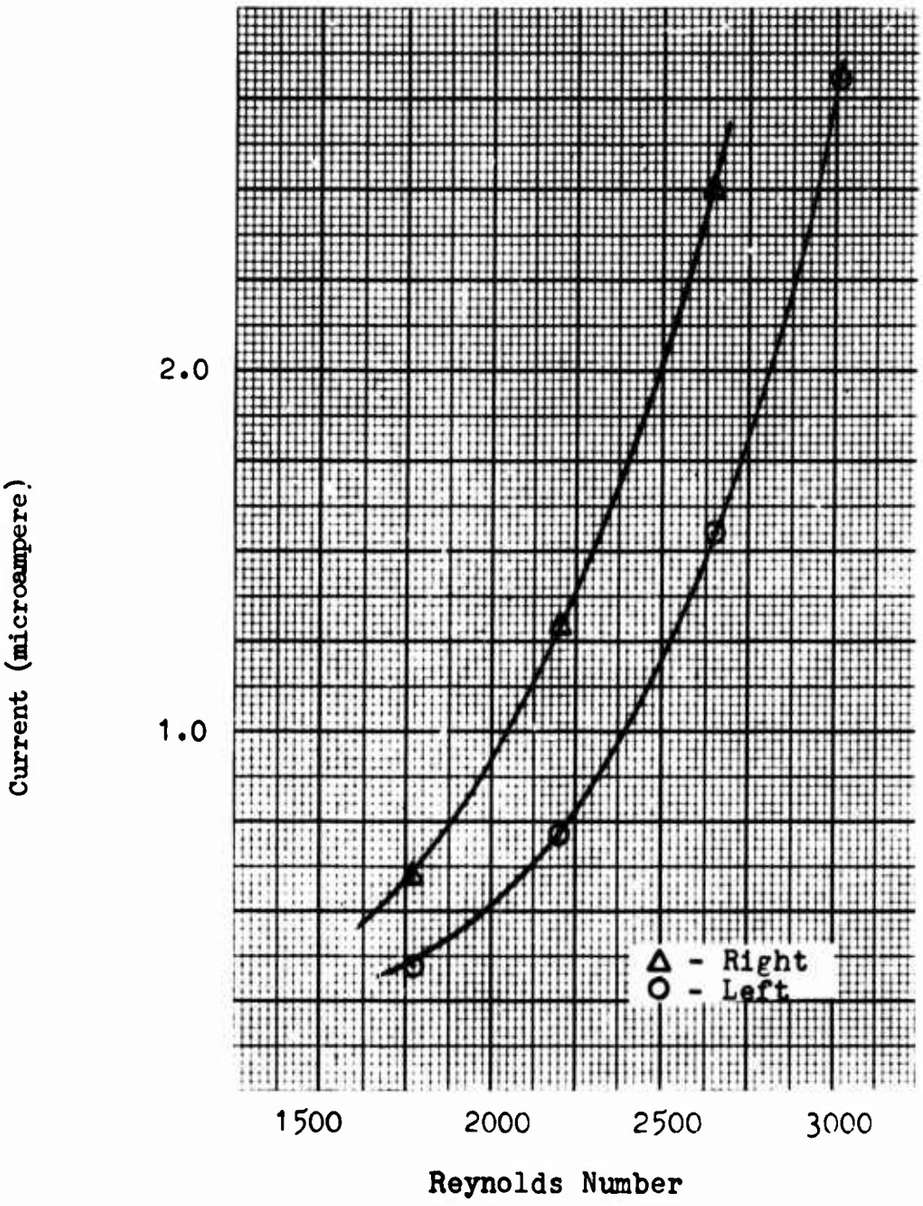

Fig. 25 - Current required to flip flow for various Reynolds numbers. A = 3/4 inch

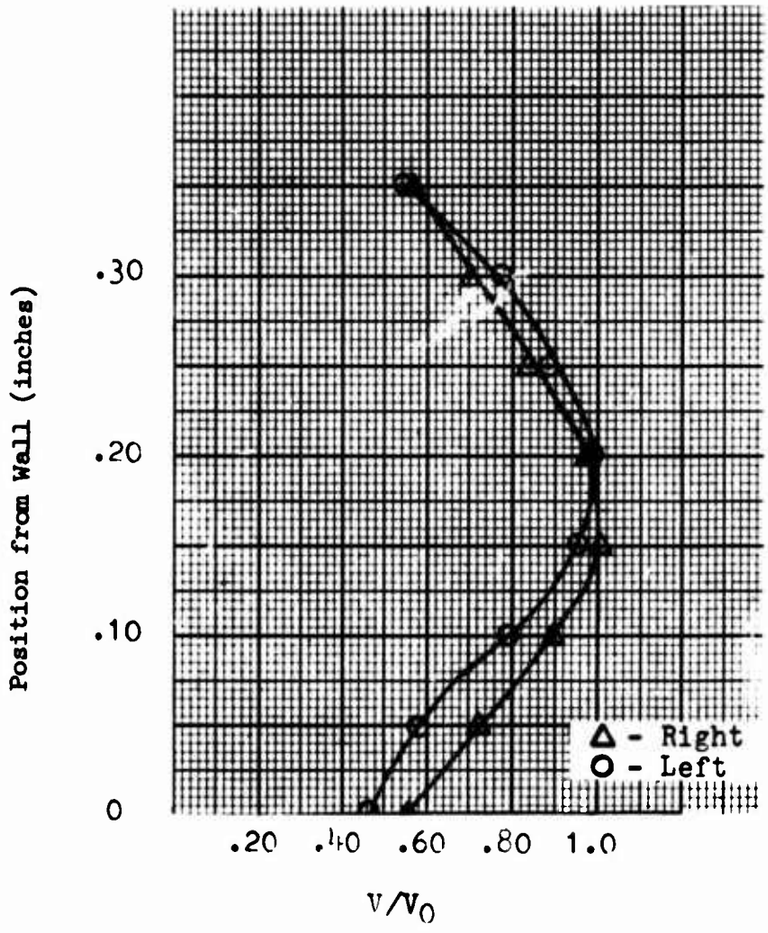

Fig. 26 - Velocity profile before and after flipping. Reynolds number = 2640

Figure 27

Description of Test 2

Positive Electrode	0.008-inch steel wire
Negative Electrode	1/4 x 3/16 x 1/32-inch brass plates
Distance Between Electrodes, A	3/4 and 1 inch
Amplifier	No. 2
Flow Channel Angle	10°
Interaction Width	0.20 inch
Splitter Position, s	no splitter
Current	0-3 microampere
Voltage	0-22 kilovolts
Reynolds Number	2800-4400

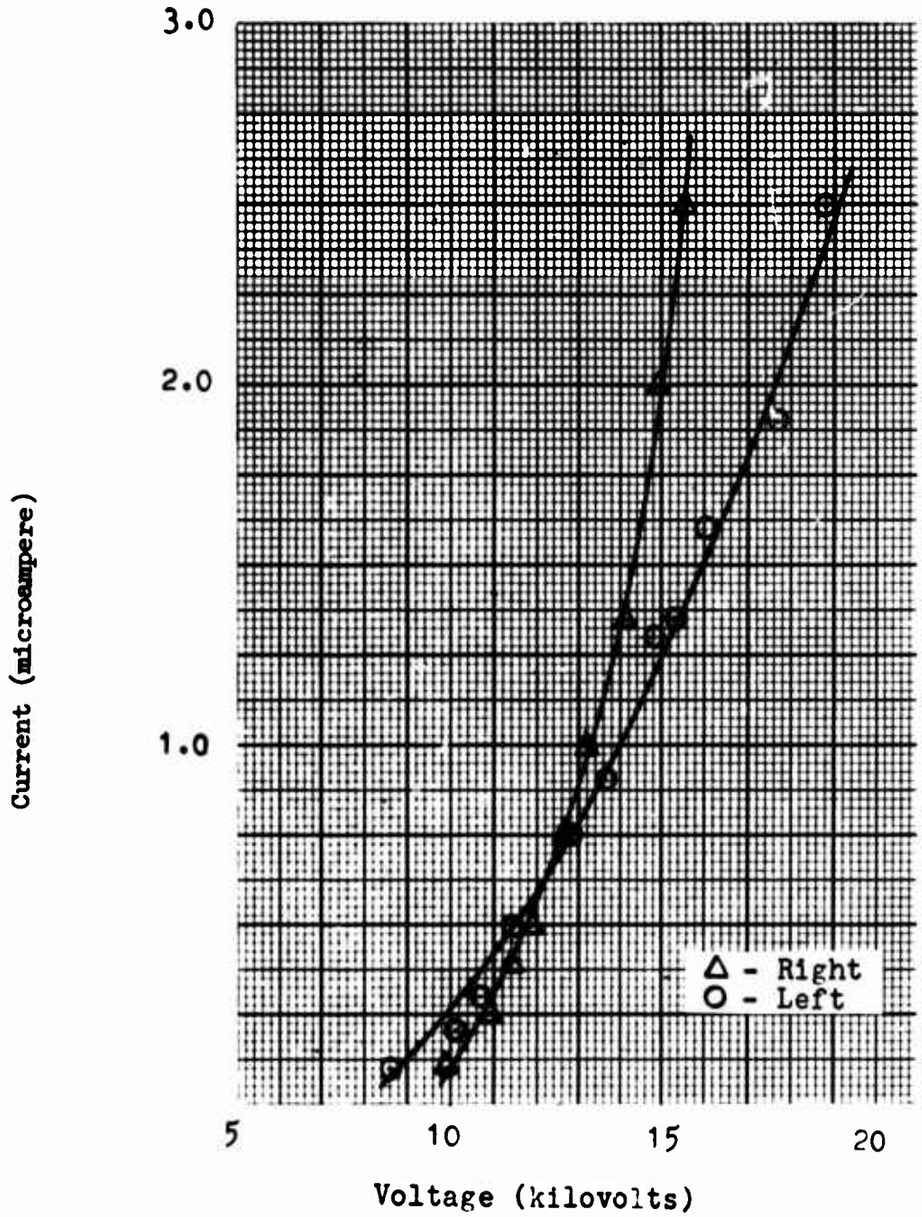

Fig. 28 - Current-voltage relation. A = 1 inch

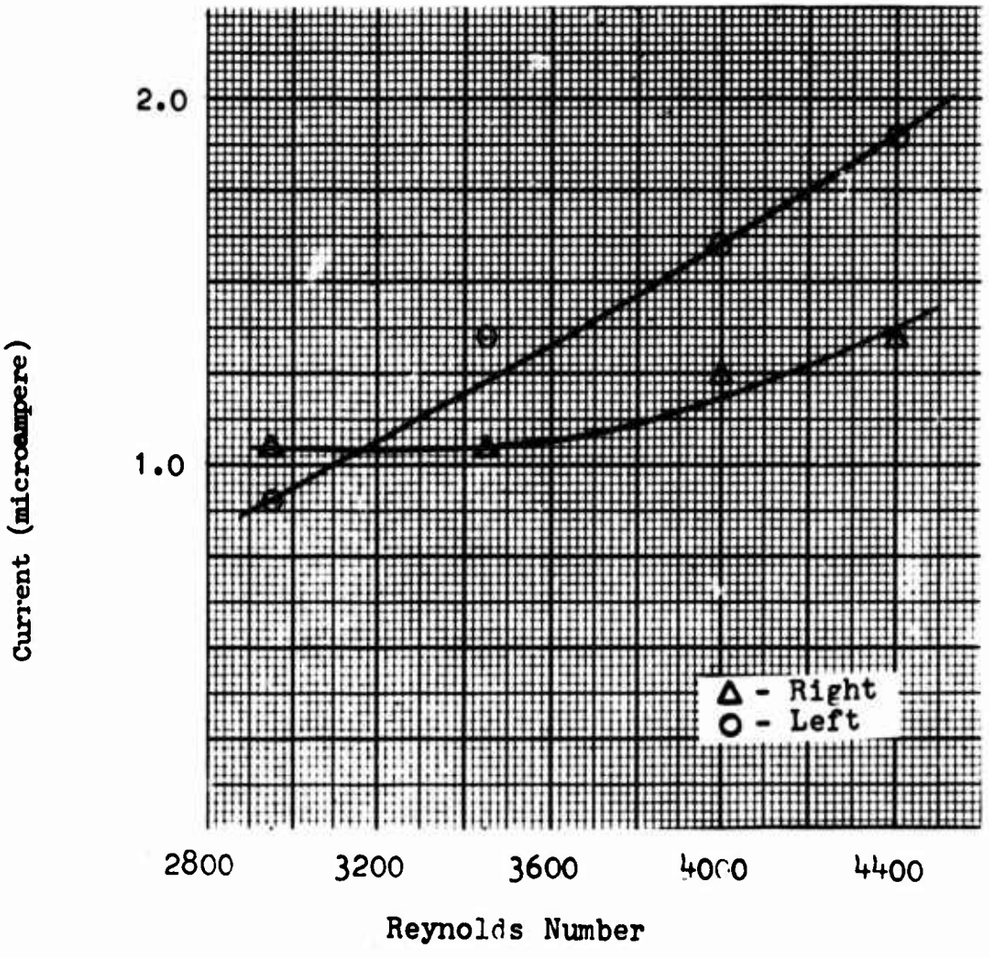

Fig. 29 - Current required to flip flow for various Reynolds numbers. A = 1 inch

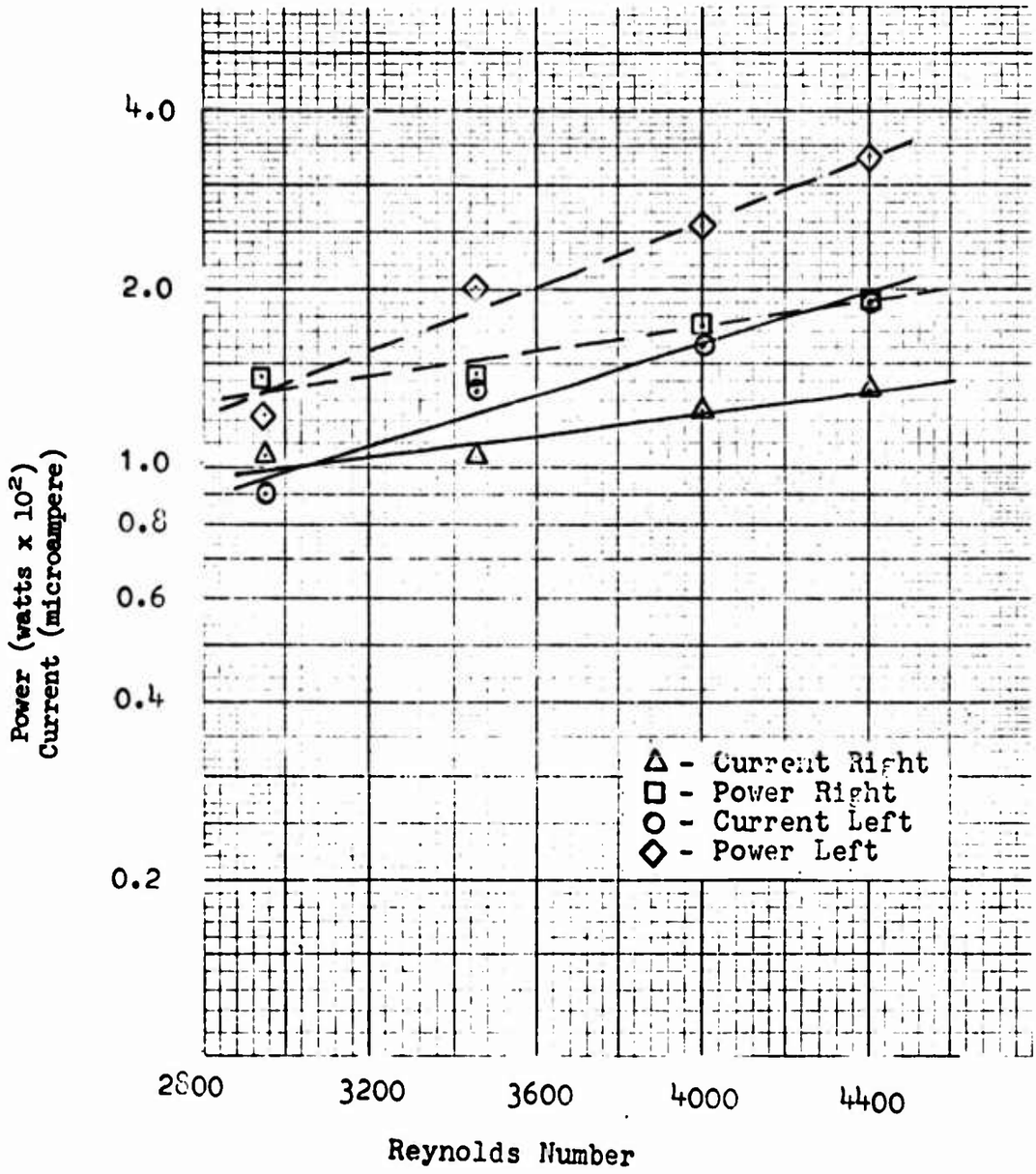

Fig. 30 - Power and current required to flip flow both ways for various Reynolds numbers. A = 1 inch

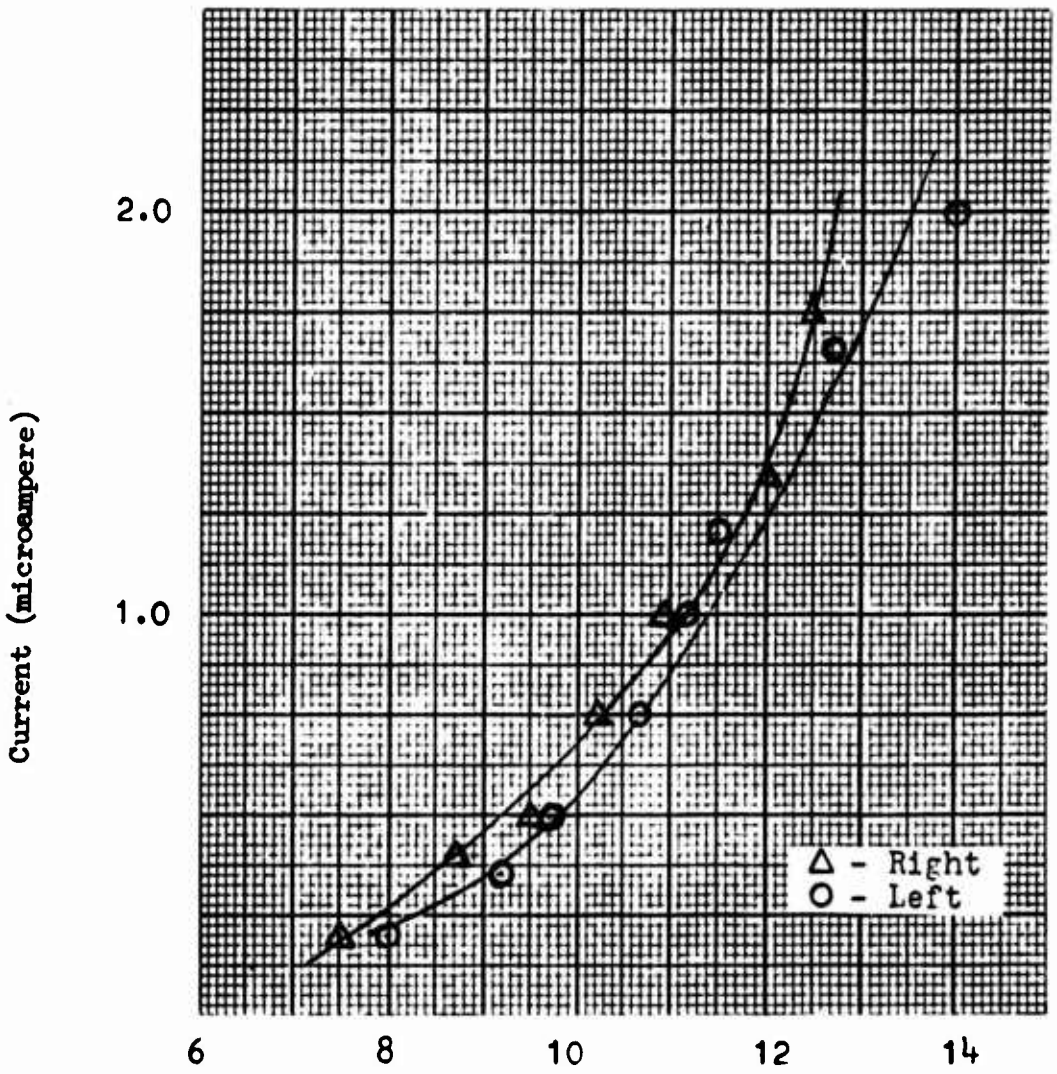

Fig. 31 - Current-voltage relation. A = 3/4 inch

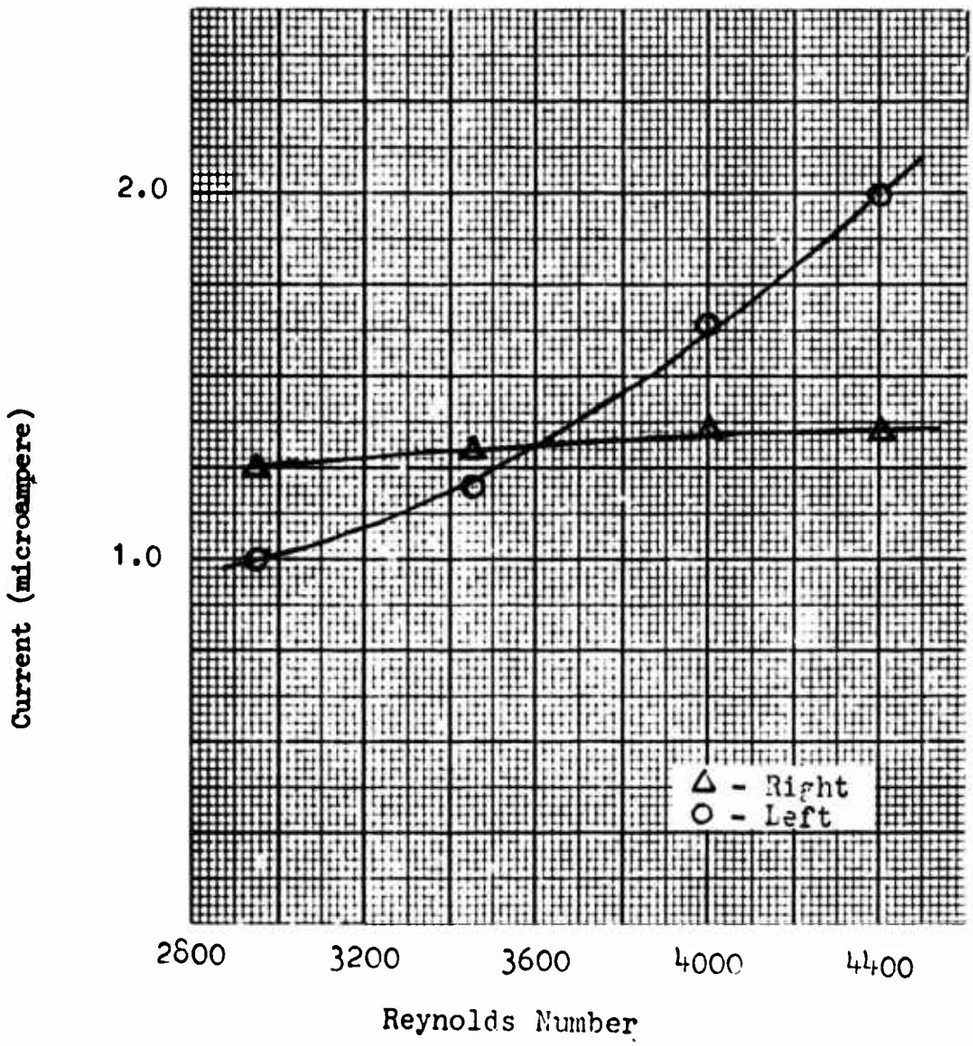

Fig. 32 - Current required to flip flow for various Reynolds numbers. A = 3/4 inch

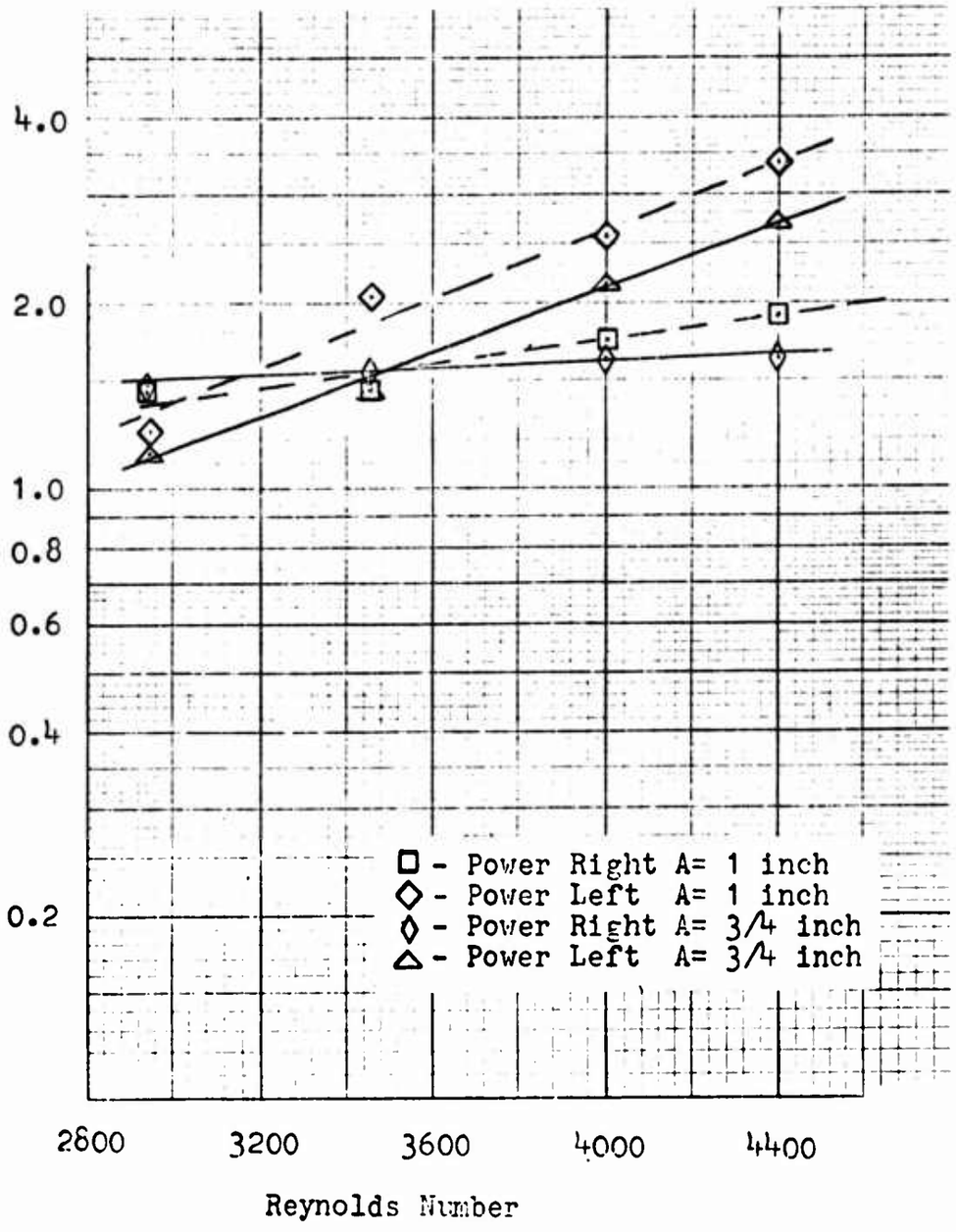

Fig. 33 - Power required to flip flow both ways for different corona point positions and various Reynolds numbers

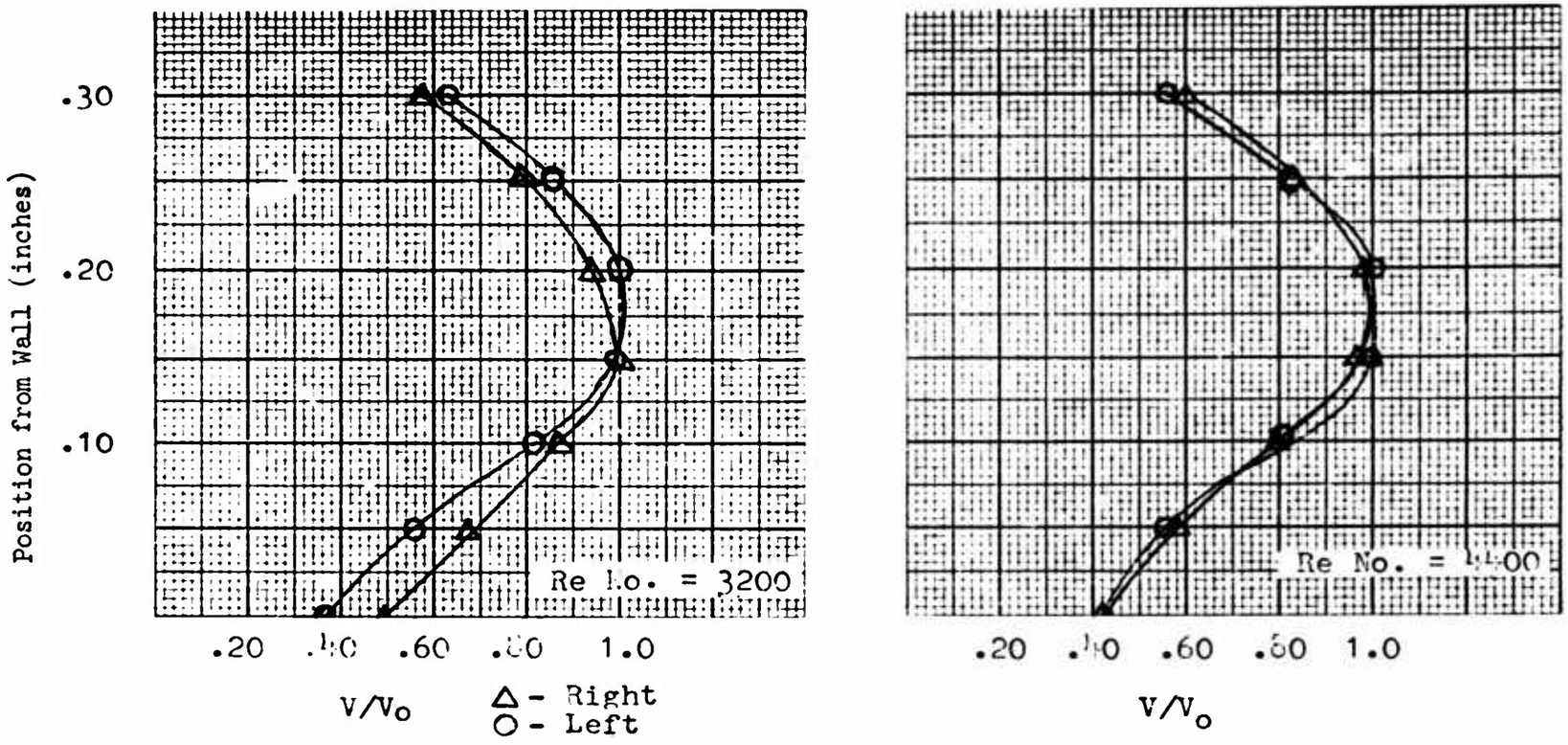

Fig. 34 - Velocity profiles before and after flipping

Figure 35

Description of Test 3

Positive Electrode	0.008-inch steel wire
Negative Electrode	1/4 x 3/16 x 1/32-inch brass plates
Distance Between Electrodes, A	3/4 and 1 inch
Amplifier	No. 3
Flow Channel Angle	20°
Interaction Width	0.30 inch
Splitter Position, s	1.00 inch
Current	0-3 microampere
Voltage	0.19 kilovolts
Reynolds Number	2800-3650

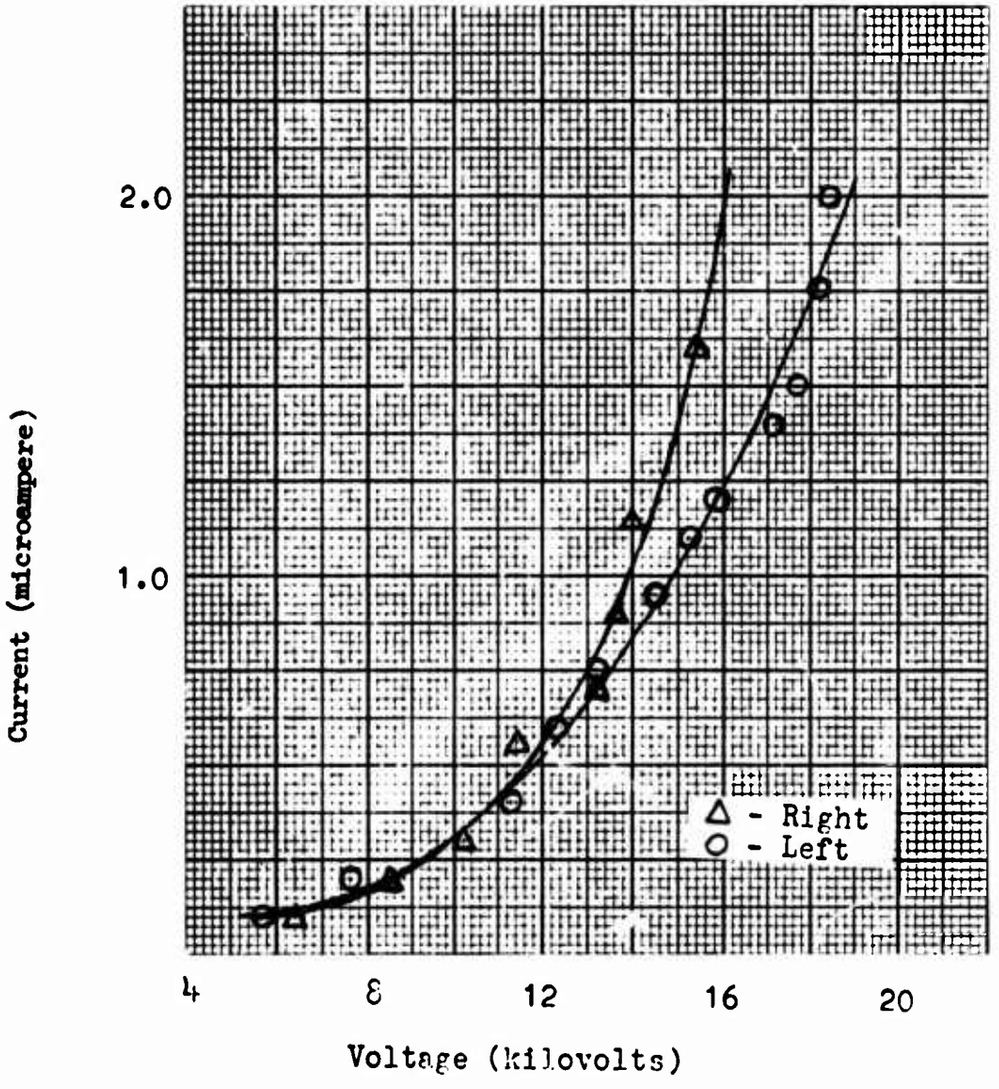

Fig. 36 - Current voltage relation. A = 1 inch

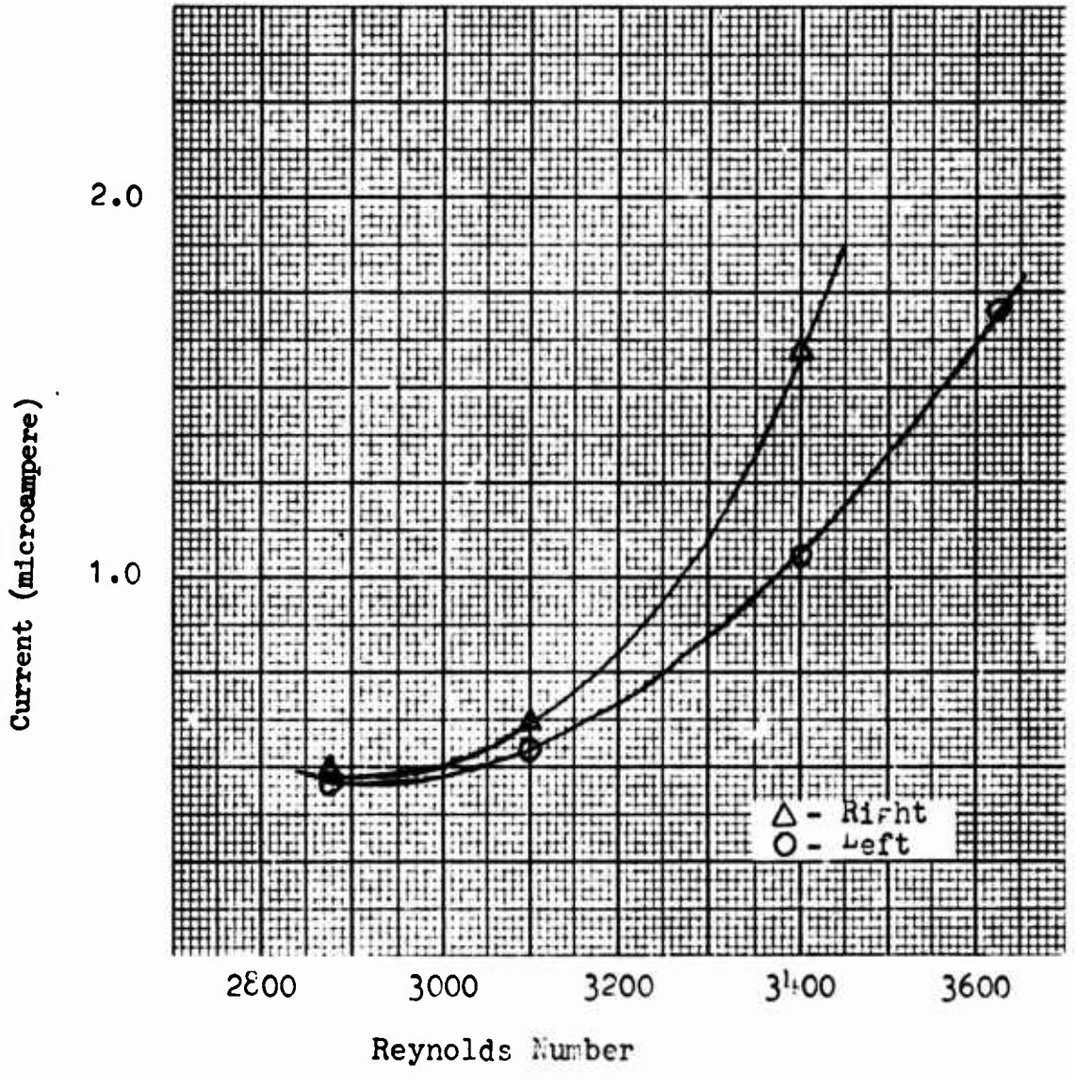

Fig. 37 - Current required to flip flow for various Reynolds numbers. A = 1 inch

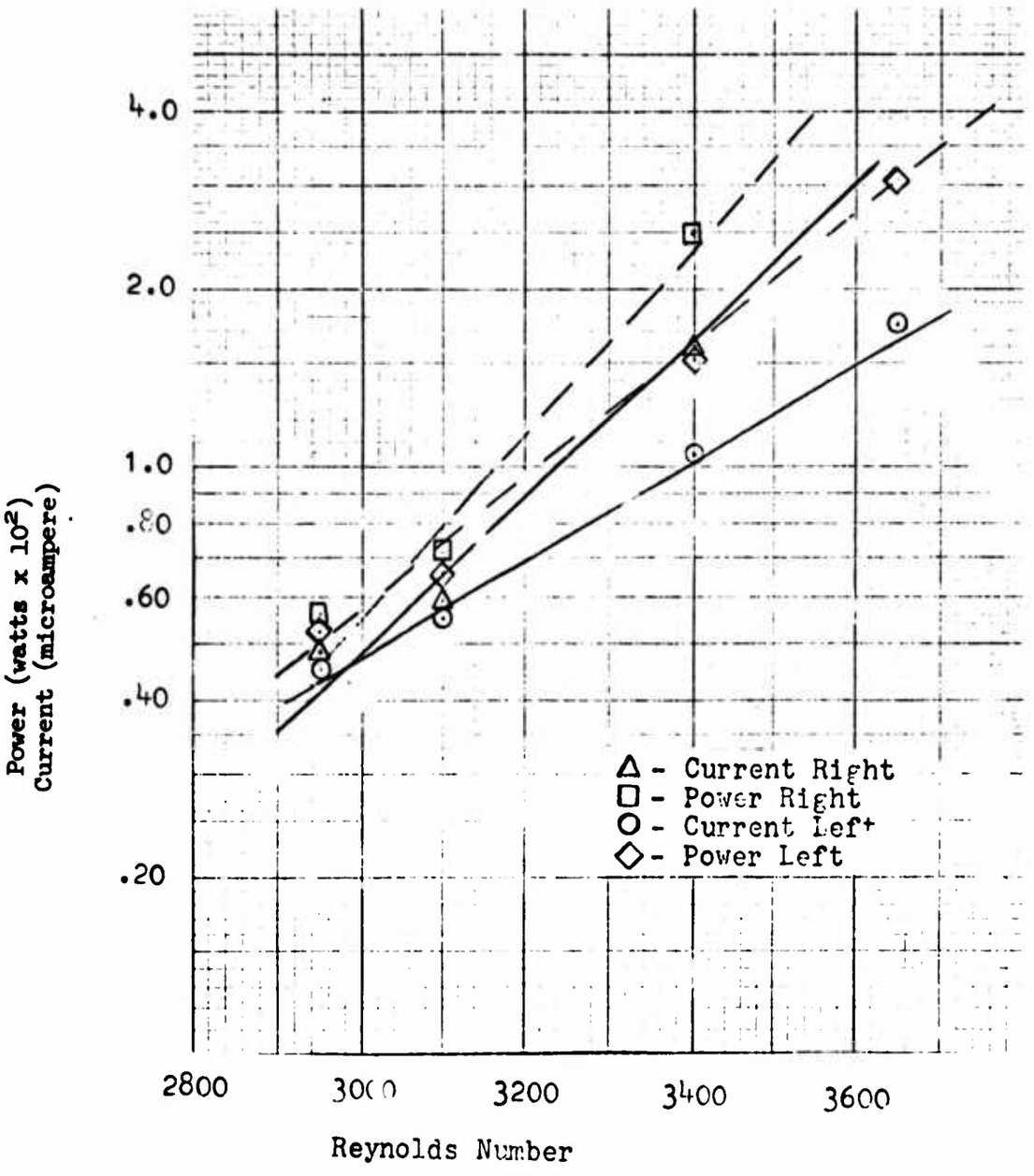

Fig. 38 - Power and current required to flip flow both ways for various Reynolds numbers. A = 1 inch

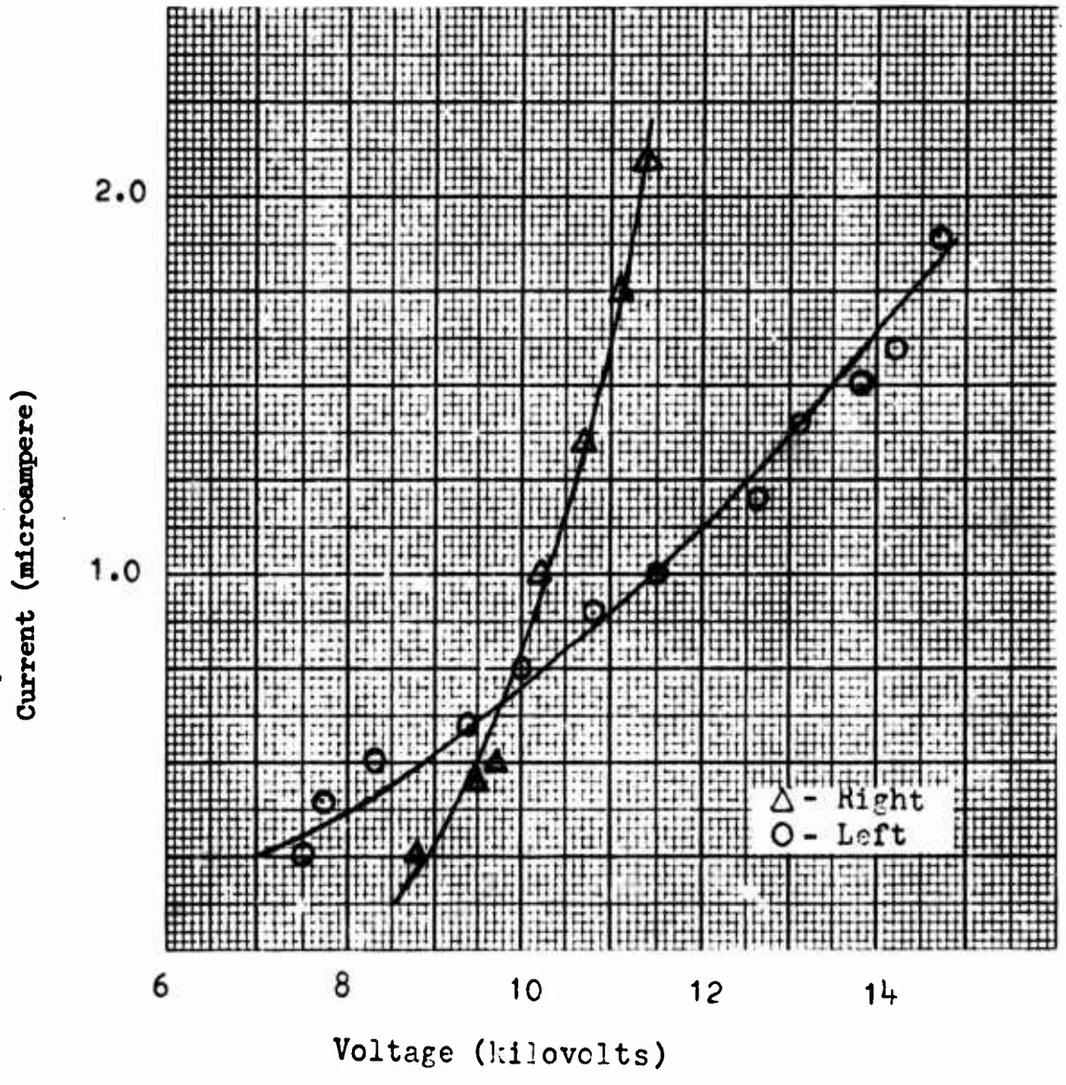

Fig. 39 - Current-voltage relation A = 3/4 inch

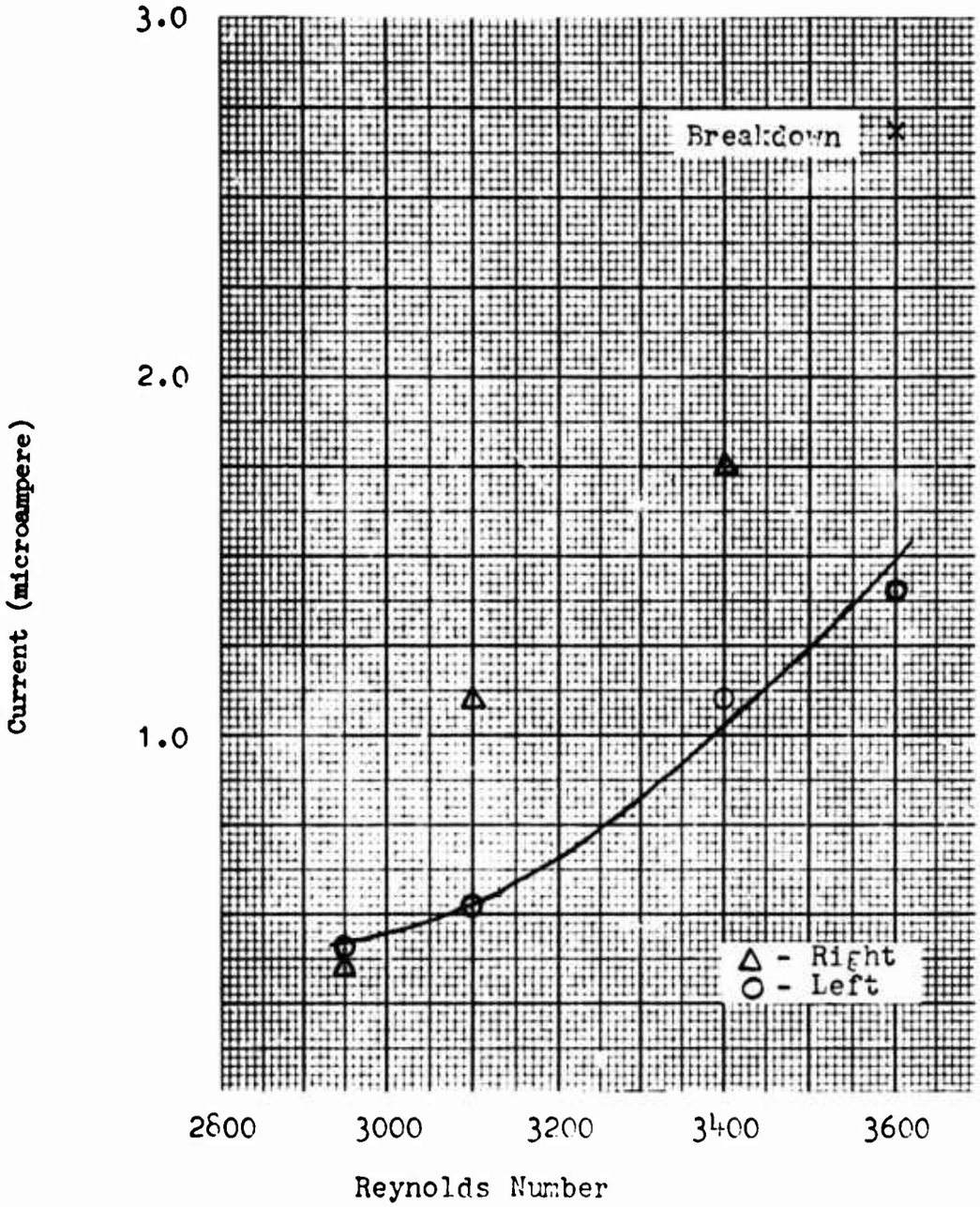

Fig. 40 - Current required to flip flow for various Reynolds numbers. A = 3/4 inch

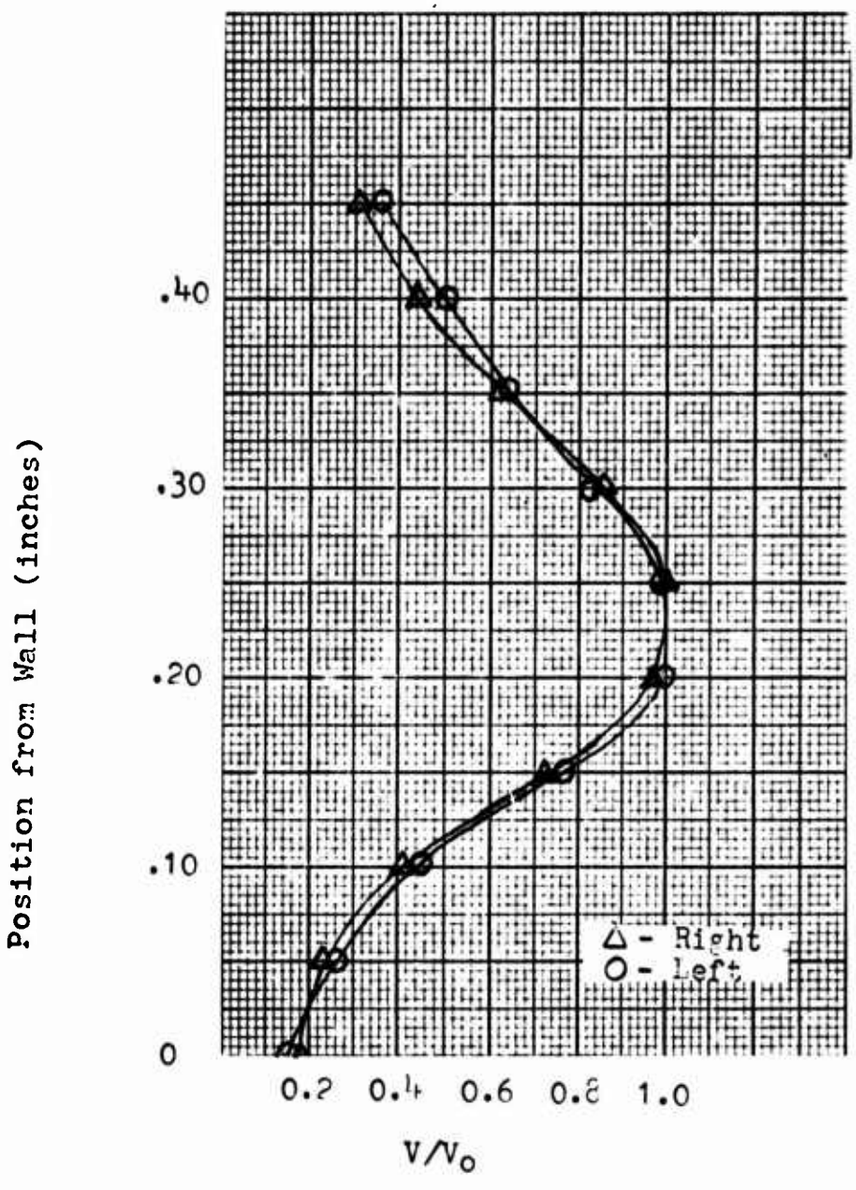

Fig. 41 - Velocity profile before and after flipping. Reynolds number = 3400

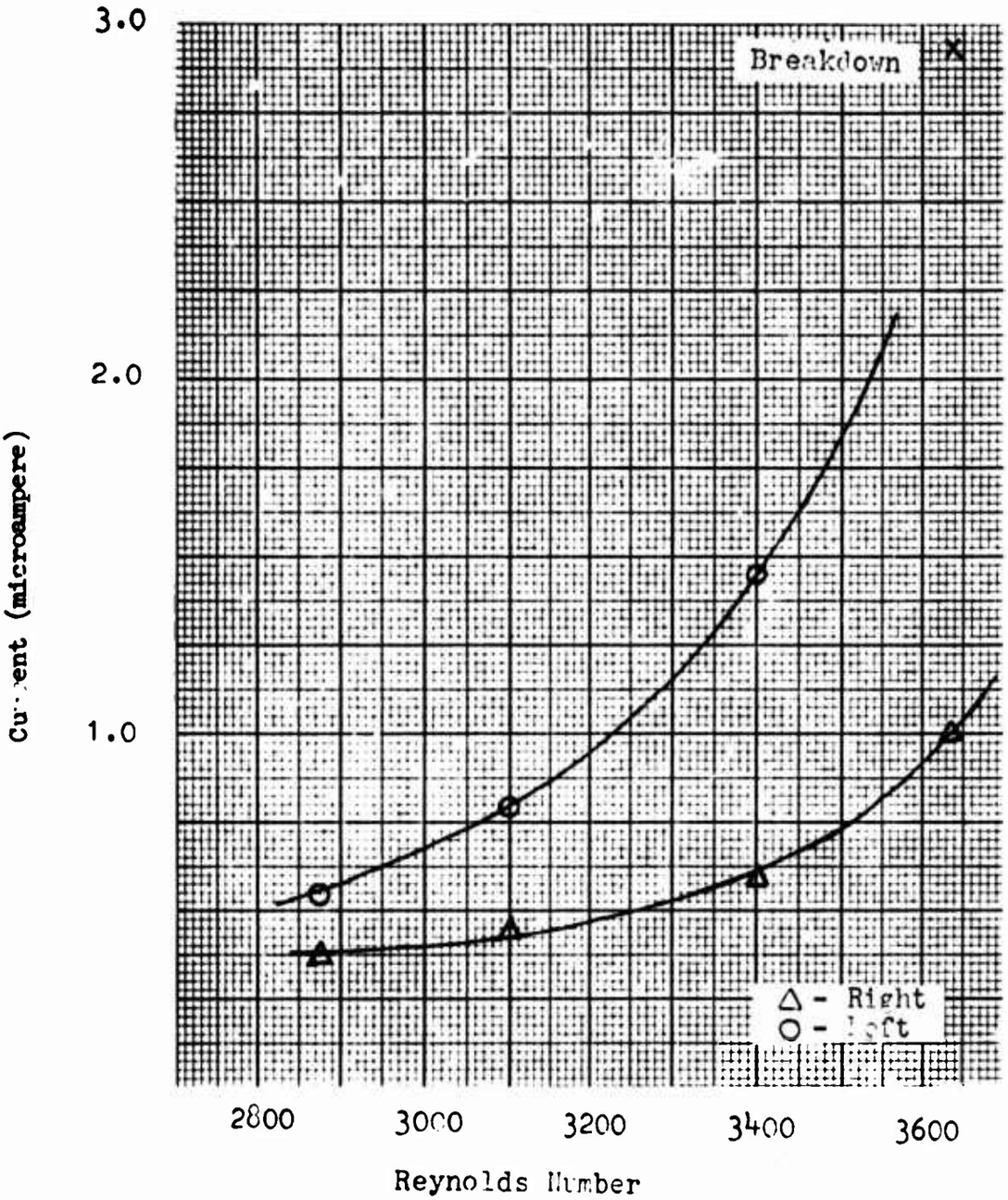

Fig. 42 - Current required to flip flow for various Reynolds numbers. A = 1 inch
Right side of channel offset 0.04 inch

Figure 43

Description of Test 4

Positive Electrode	0.008-inch steel wire
Negative Electrode	1/4 x 3/16 x 1/32-inch brass plates
Distance between Electrodes, A	1 inch
Amplifier	No. 1
Splitter Position, s	1.00 inch
Current	0-1.5 microampere
Voltage	0-18 kilovolts
Reynolds Number	2150
Hoses	Tygon tubing, 3/8 inch O.D. 1/4 inch I.D., 12-1/2 inch long
Plenum Chamber	Quart can with removable top

Table I. Current and Voltage Required to Flip Flow
(Reynolds Number = 2150)

Control Port Condition	Left		Right	
	Current (microampere)	Voltage (kilovolt)	Current (microampere)	Voltage (kilovolt)
Open, Fig. 8	0.90	15.1	0.55	12.9
Hoses, (not connected)	1.20	17.4	0.87	15.2
Hoses (connected) Fig. 18	1.10	16.8	0.80	14.6
Hoses and Plenum (Top closed) Fig. 19	1.30	18.0	1.50	16.7
Hoses and Plenum (Top open)	1.30	17.8	1.45	16.5

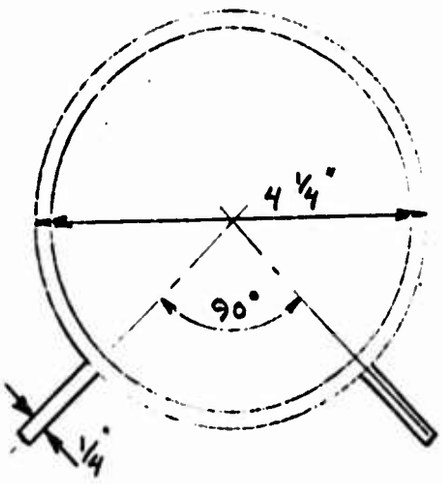

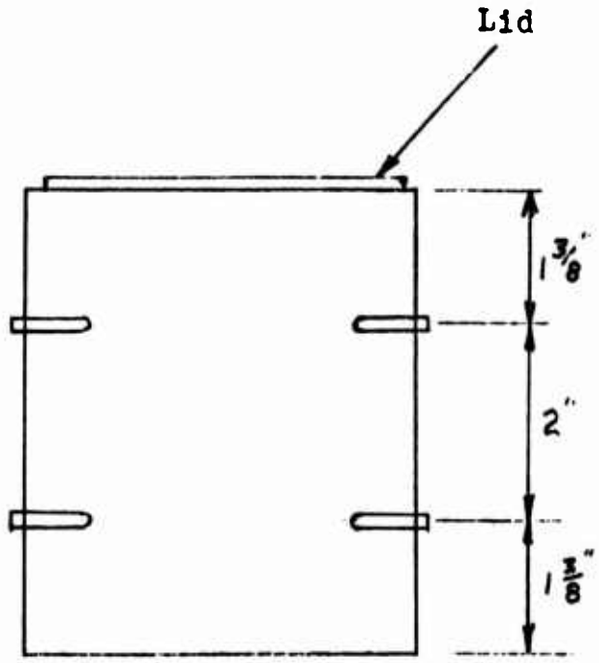

Fig. 44 - Diagram of plenum chamber

Figure 45

Description of Test 5

Control Port Velocity Test

Positive Electrode	0.008-inch steel wire
Negative Electrode	1/4 x 3/16 x 1/32-inch brass plates
Distance between Electrodes, A	1 inch
Current	0.75, 1.00, and 1.25 microampere

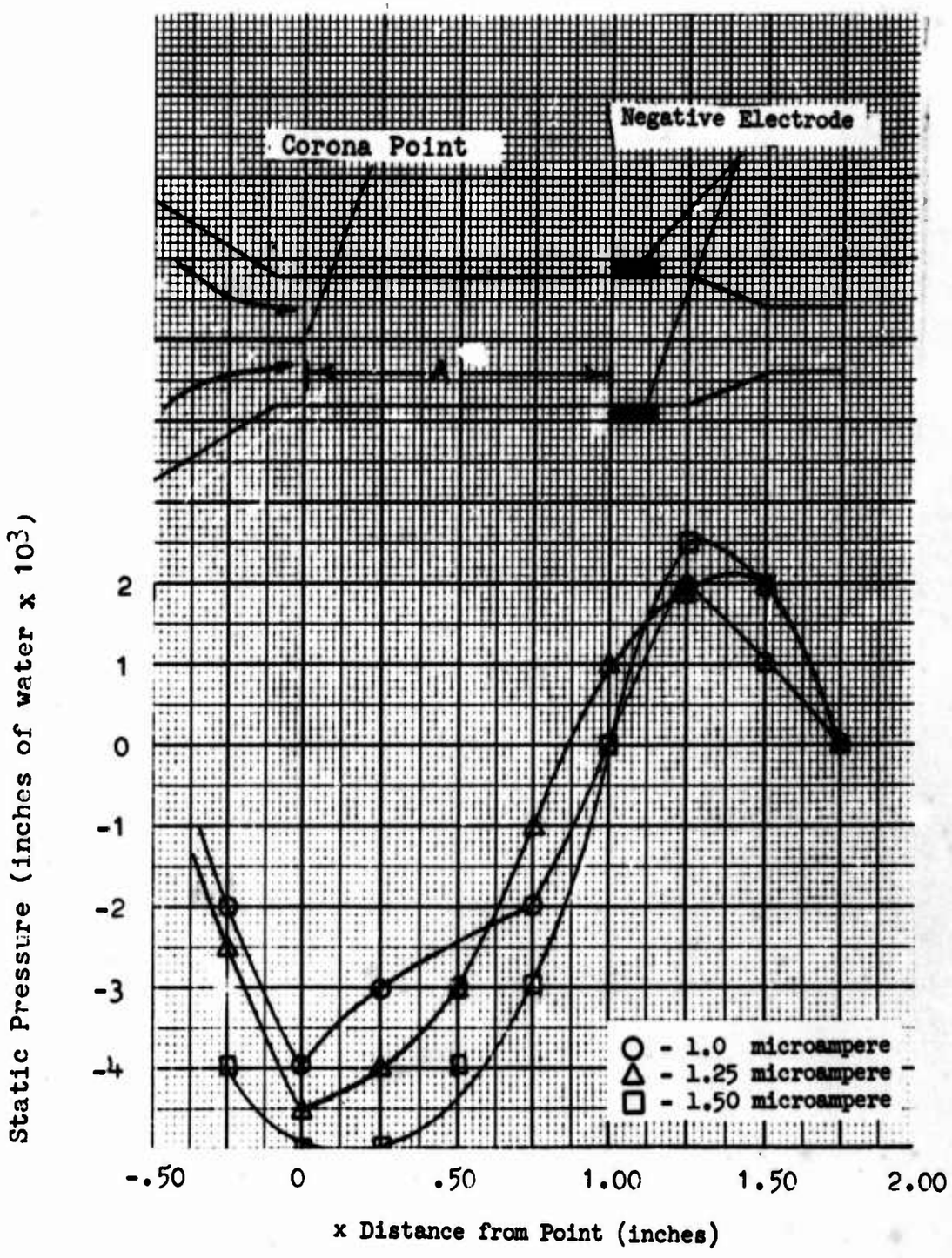

Fig. 46 - Static pressure variation along control port at various currents

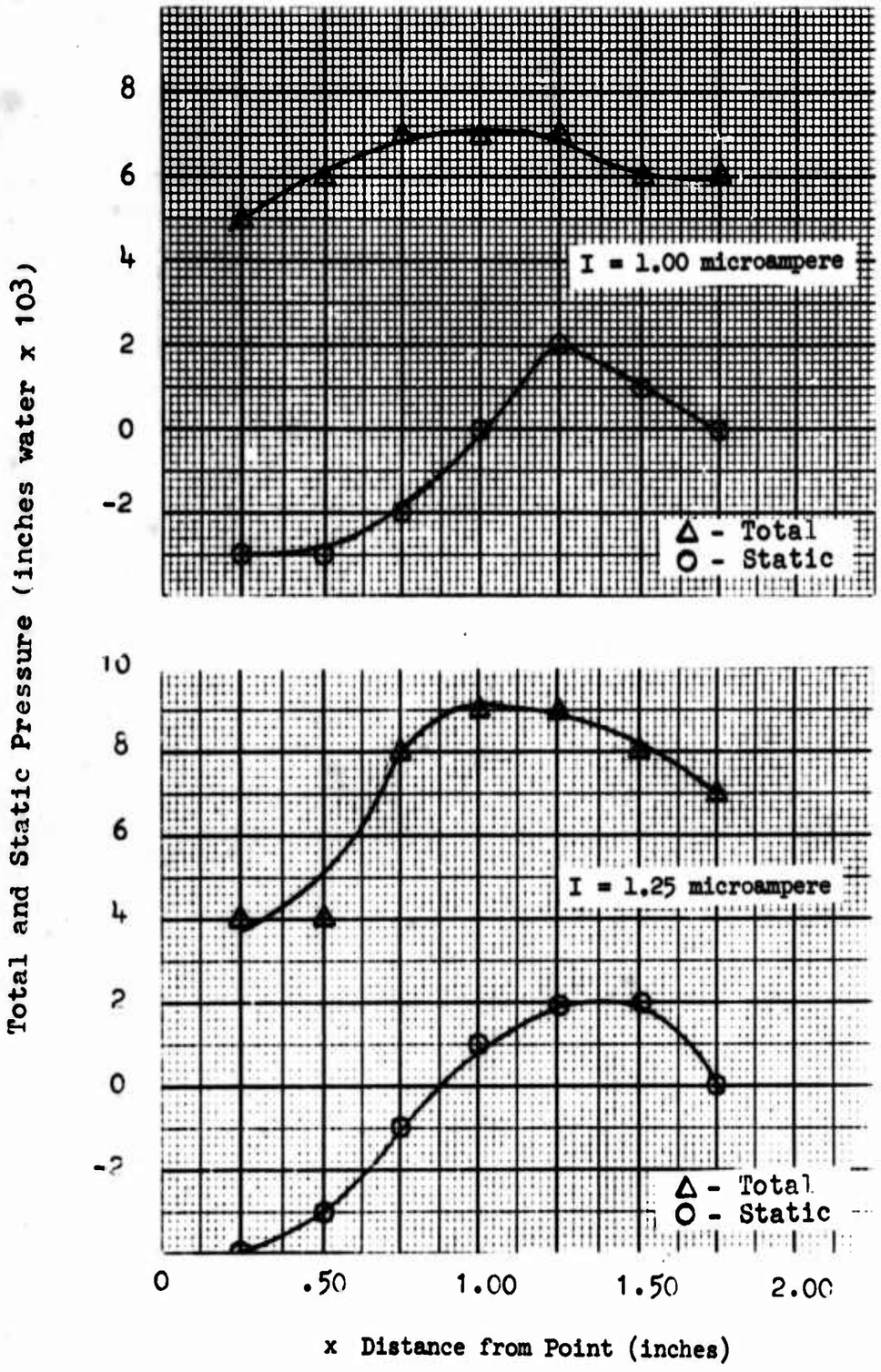

Fig. 47 - Total and static pressure variation along control port at various currents

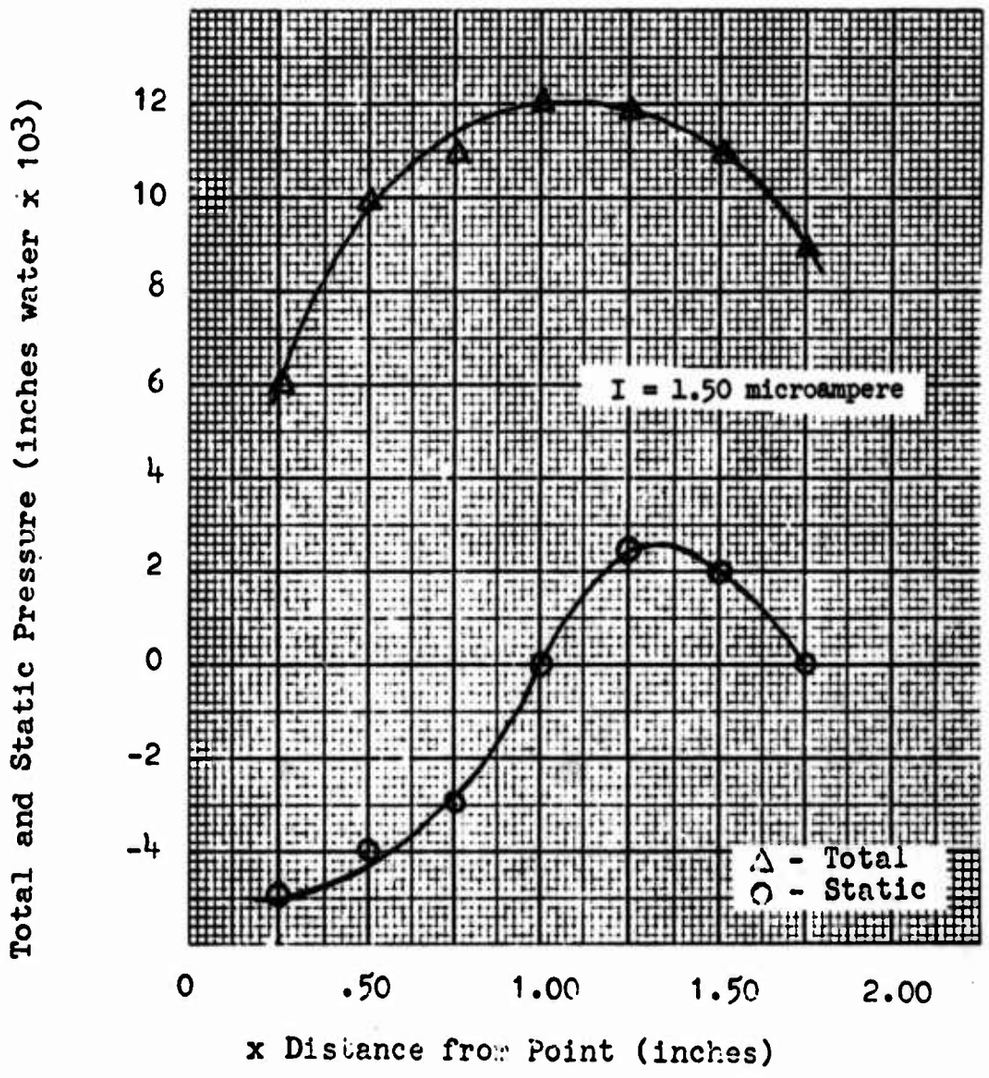

Fig. 48 - Total and static pressure varation along control port at various currents

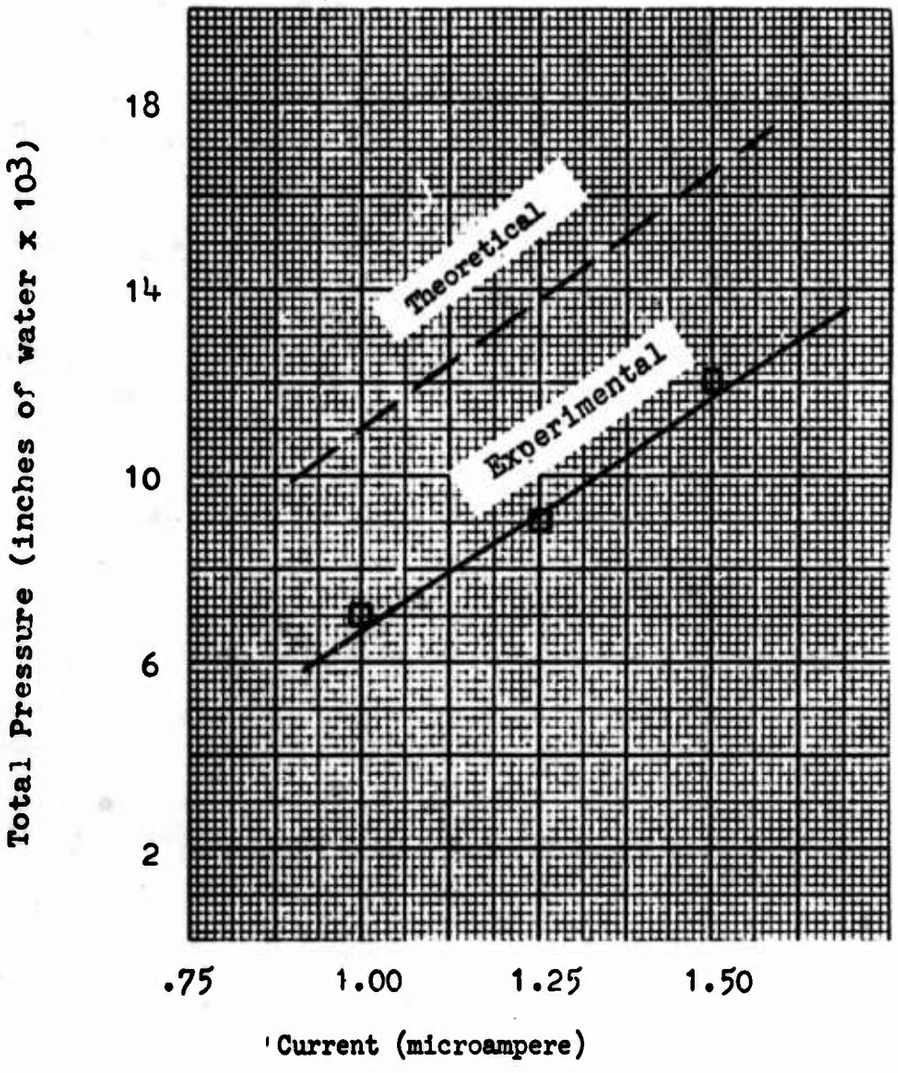

Fig. 49 - Total pressure increase at electrodes for various currents

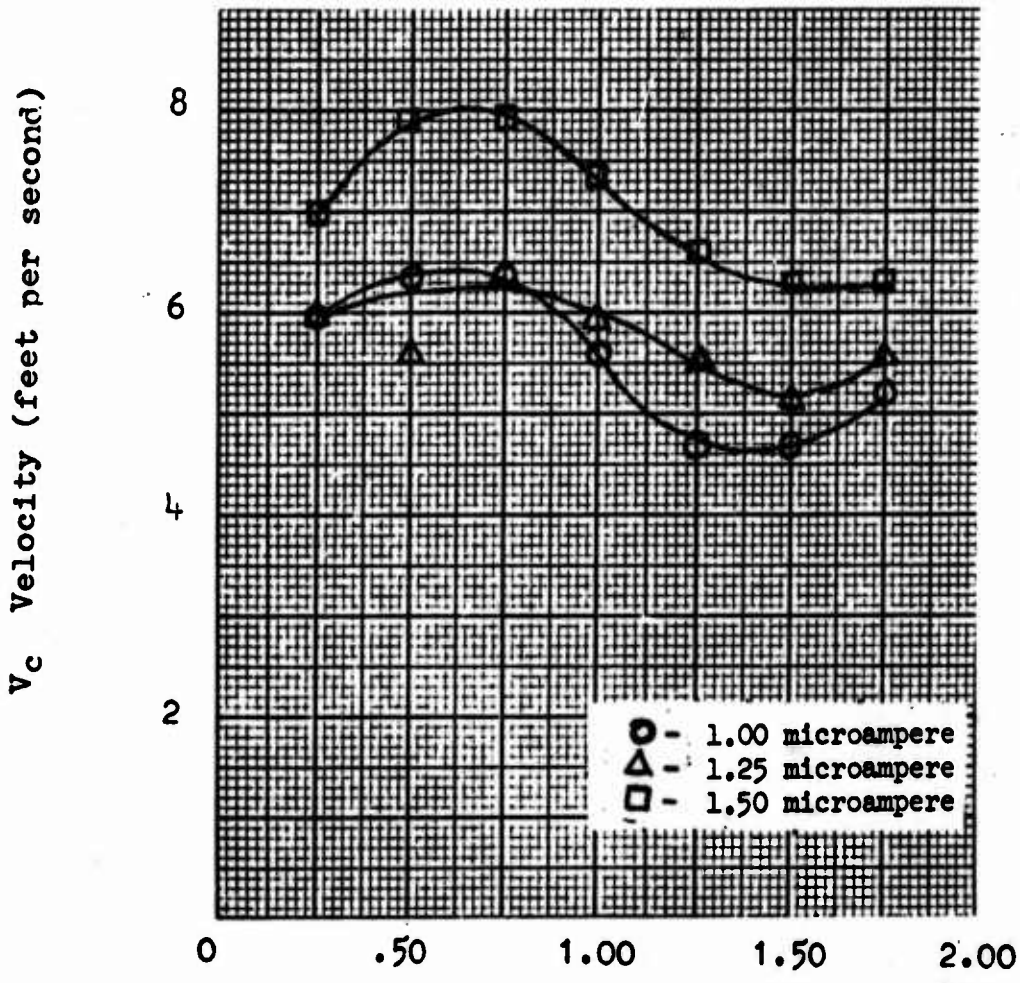

Fig. 50 - Velocity along control port at various currents

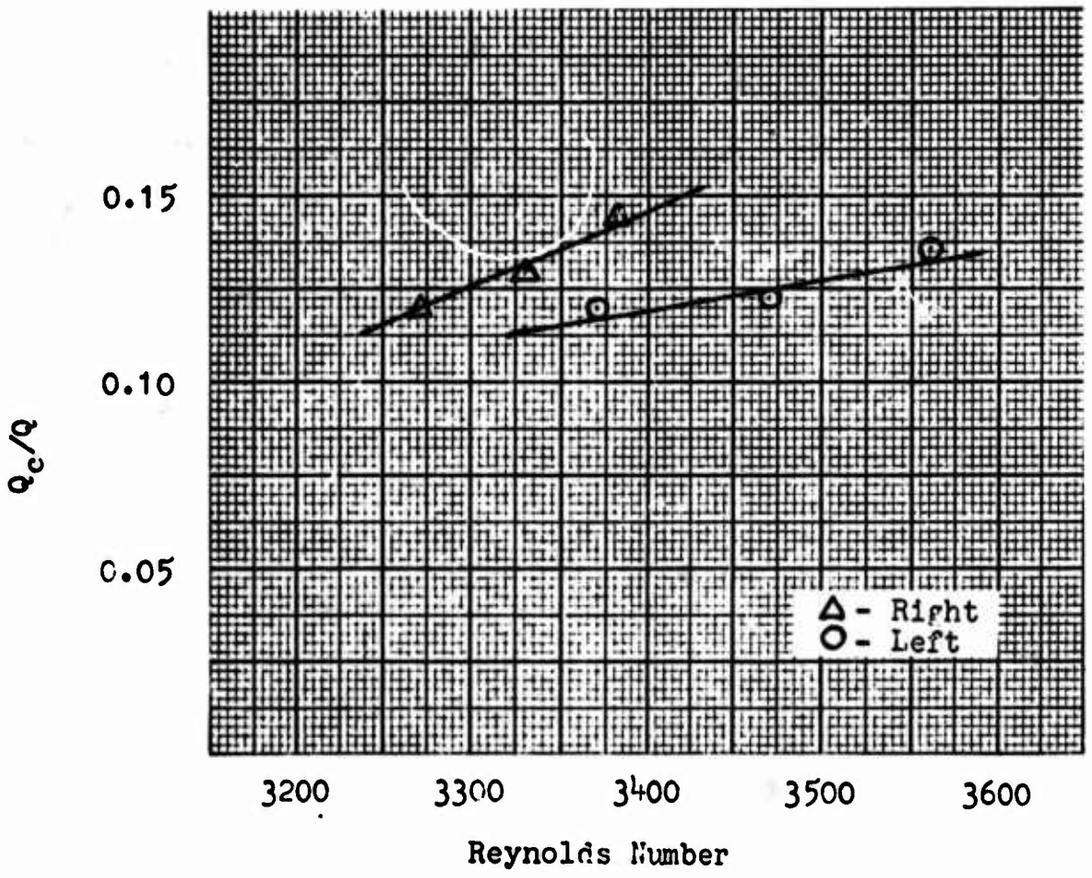

Fig. 51 - Q_c/Q for various Reynolds numbers. Amplifier No. 3. A = 1 inch

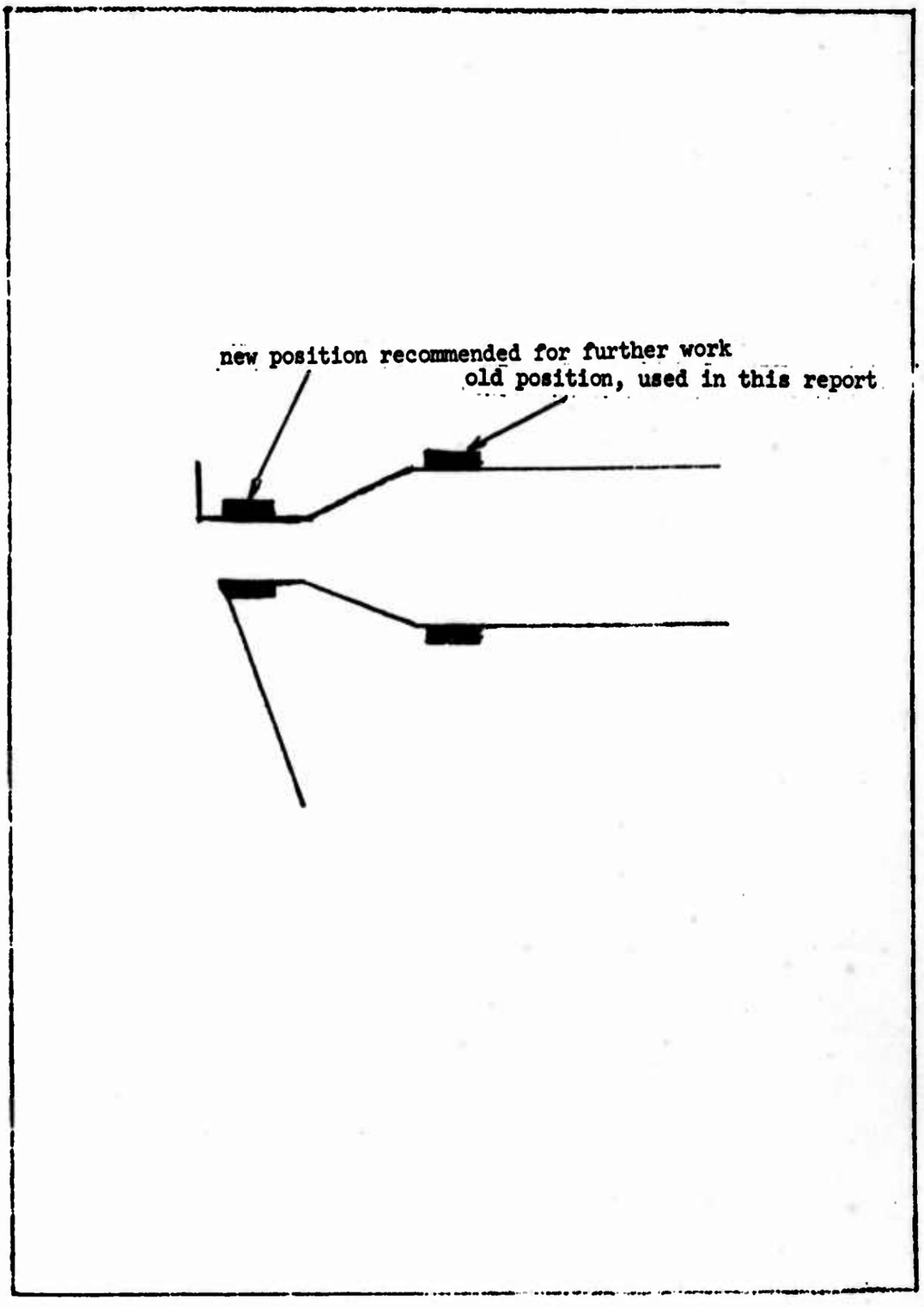

Fig. 52 - Positions of negative electrodes

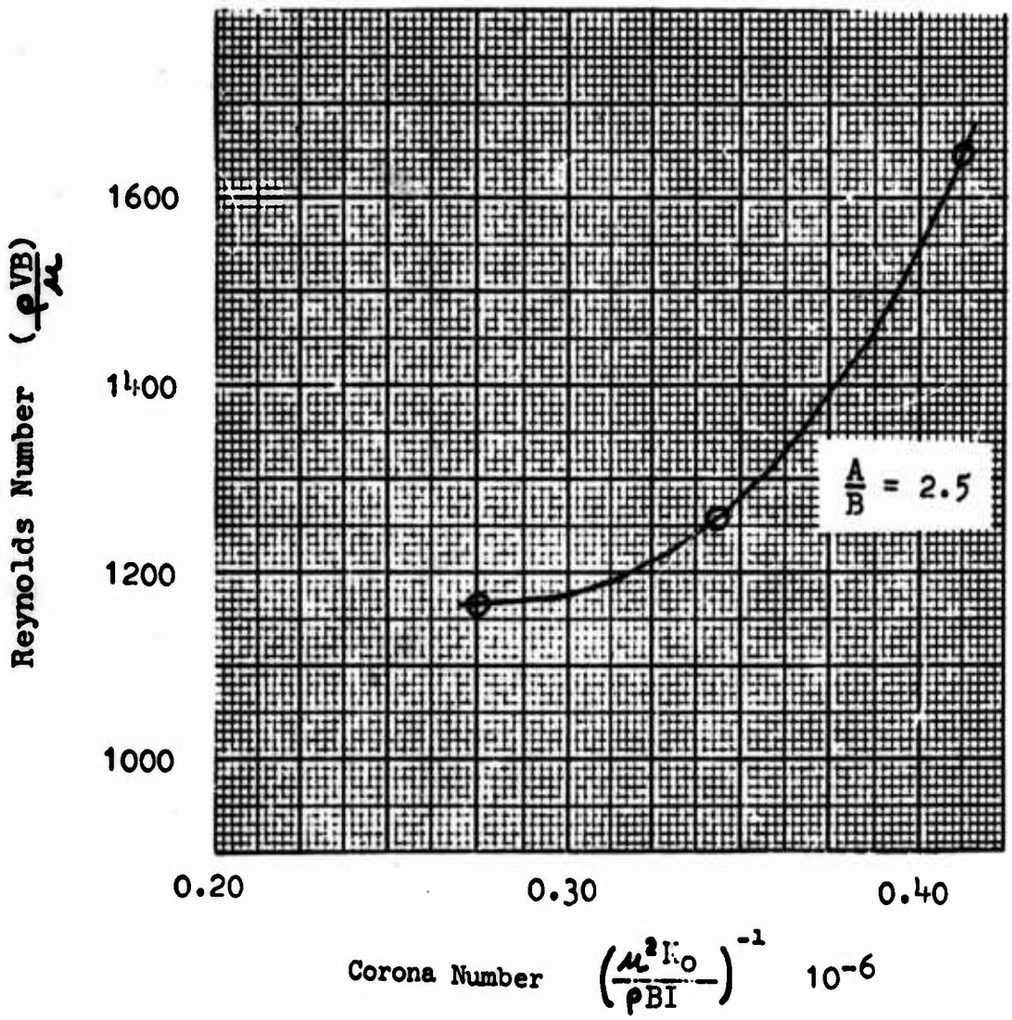

Fig. 53 - Control port Reynolds numbers for various corona numbers

EXPERIMENTAL CALCULATIONS

Nozzle Reynolds Number

The Reynolds number based on the nozzle width, w, and the mean nozzle velocity, V_n, is given by

$$Re = \frac{\rho V_n w}{\mu} \tag{1}$$

From Bernoulli's equation

$$p_t - p_s = 1/2(\rho V_n^2) \tag{2}$$

$$V_n = \sqrt{2(p_t - p_s)/\rho} \tag{3}$$

Combining Eqs. (1) and (3)

$$Re = \frac{w}{\mu}\sqrt{2(p_t - p_s)\rho} \tag{4}$$

Channel Velocity

The same procedure was used here as in the Reynolds number calculation.

$$V = \sqrt{2(p_t - p_s)/\rho} \tag{5}$$

where p_t is the total pressure at the channel exist.

Calling the maximum velocity in the channel V_o, plot the dimensionless parameter.

$$\frac{V}{V_o} = \sqrt{\frac{pt - ps}{pto - pso}} \tag{6}$$

III. RESULTS OF EXPERIMENTAL INVESTIGATION

LARGE AMPLIFIER

The large amplifier was modified from its initial design, Fig. 14, to incorporate the addition of a plenum chamber. The hoses and plenum chamber were added to the existing amplifier, Fig. 15, as a means of regulating the flow of air through each control port. A five-gallon can was used for the chamber with two one-half inch pipe nipples welded on the side for inlets. To seal off the amplifier, two wooden nozzles were made to contour fit the existing parts for a tight seal. One-half inch rubber hoses were used to connect the control ports and plenum chamber, and valves were mounted to regulate the flow.

Preliminary tests with just the hoses connected showed that the flow could be flipped but only with a very high current. There was also considerable current leakage through the wood nozzles to the flow channel plates. Varnishing the wood to improve insulation qualities did not improve the problem.

The hoses were hooked up to the plenum chamber and the channel plates were grounded. At all Reynolds numbers the flow could not be switched, probably because of the increased resistance to air flow from the can. Sparking would always occur before enough wind could be generated to flip the flow.

Plexiglas nozzles were substituted in place of the wooden nozzles to see if the better insulating qualities would stop the current leakage. The leakage was cut down noticeably, but this did not help in getting the flow to flip. It was obvious that the amplifier required more electrical power for flipping than was available to the present configuration. The large amplifier was abandoned at this point in favor of a new more compact design.

DESIGN OF MINIATURE MODEL

The design of a new amplifier on a smaller scale was based on the proven principles of geometry that have been successful in operational amplifiers.[6,7] The design limitation was in the control port size since a maximum amount of wind was an immediate goal and breakdown was a major problem in the large amplifier control port.

The dimensions of the control port were selected on the basis of the channel thickness and the rest of the amplifier was designed to proportionally fit the control port. When tests on Amplifier No. 1 were encouraging, two more amplifiers were built with the same size control ports but with different size flow channels.

CURRENT-VOLTAGE RELATIONSHIP

For each test condition, the current flowing between the electrodes was plotted against the voltage. A slight change in the position of the corona wire or a burnt-out tip would cause a change in the current-voltage relation so the relation was recorded for each test.

Each current-voltage plot assumed approximately the same shape. As the voltage increased, the current would increase slowly at first, but would begin a sharp increase and approach a vertical line at higher voltages. At high voltages there was a greater tendency for breakdown (sparking) to occur. This would often happen without a visible spark, but the current would jump up to ten times the value before breakdown. Extreme care had to be taken to ensure the ammeter would not be damaged. Once breakdown had occured, sparking would still repeat at lower voltages than before. Only by turning down the voltage and waiting a few seconds could the voltage be turned up again without sparking.

Tests were also run with the lights out and the sparking that was not visible before could be seen. During the first tests the discharge was always to one corner of the negative electrode and occurred at low voltages. This corner was protruding slightly from the wall of the control port although it should have been flush. After filing the plate flush with the wall, this premature discharge did not occur again.

All of the tests were run with a positive corona, that is, a positive charge on the needle point. A negative corona was used but no appreciable difference was noted. For an explanation of positive and negative corona, see Appendix I.

CURRENT REQUIRED TO FLIP FLOW

In Test 1 the flow was flipped each direction with about the same current at the lowest Reynolds number, but at higher Reynolds numbers it took almost twice as much current to flip from right to left than from left to right (Figs. 22 and 25). This was true for each distance A, but the difference was not as pronounced for A = 3/4 inch. When the Reynolds number exceeded 3000, breakdown would occur before the flow would flip.

For Test 2 the current to flip the flow from right to left does not change much through the whole range of Reynolds numbers, yet it follows a steadily increasing pattern for flipping from left to right much the same as in Test 1. In comparing both runs, A = 3/4 and A - 1 inch, the current to flip was just slightly more for the case when A = 3/4 inch, but the voltage was considerably smaller (Figs. 31 and 32). This means that less power was required to produce a sufficient wind for flipping when the point was closer to the electrode as shown in Fig. 33.

In Test 3 the current was again higher to flip from right to left so the positive electrodes were switched and the results were practically the same, thus the condition of the electrodes was not much of a factor in the discrepancy between flipping currents on different sides. The flow was therefore biased to the right side because of geometry. In reassembling the amplifier with the right side of the flow channel moved away from the center of the jet to give a skewed channel (see Fig. 12), the current to flip from right to left was substantially lowered, while in the other direction it was raised, showing the pronounced effect that geometry has on the system.

The current required to flip the flow did not follow a linear pattern as the Reynolds number increased, but it did follow an approximate exponential function. Plots of both the current and power required to flip the flow left or right at various Reynolds numbers are shown in Figs. 23, 30, and 38 on semi-log paper. The equations for the different curves take the following form:[1]

$$I = C\, e^{m \cdot Re} \tag{7}$$

$$P = D\, e^{n \cdot Re} \tag{8}$$

where C and D are the intercepts of the current and power, and m and n are the slopes of the curves. For example, from Fig. 30, the current and power to flip from the right to left channel are:

$$I = 0.51\, e^{0.00023\ Re} \text{ (microampere)} \tag{9}$$

$$P = 0.0064\, e^{0.00023\ Re} \text{ (watts)} \tag{10}$$

In Test 4 different runs were made connecting parts of the plenum chamber together in succession. Amplifier No. 1 was used for this test since the results of Test 1 showed the amplifier was reliable at lower Reynolds numbers, the range in which the plenum chamber would be run, and the response to the corona wind was fast and wess defined visually, not sluggish as in the other amplifiers.

From Table I, the results showed it was more difficult to flip the flow from left to right than from right to left, and with each step, adding hoses, adding plenum chamber, etc., the current necessary to flip the flow increased. When the hoses were connected directly together, (Fig. 18) the current required was lower than every case but the open ports. In this situation the closed path between the ports acts as a plenum chamber of zero size, and gave a flipping response time that was definitely faster than with the hoses attached to the plenum chamber.

With the plenum chamber hooked up, the current was switched from one side to the other as fast as the flow would flip in the other direction. The flow would still flip at the same current as before, but the response time would slow down considerably. When the switch was thrown the initial current would be low, but would start to increase and when it reached the value necessary for flipping, the flow would flip. This caused a short delay in flipping time.

VELOCITY PROFILES

The velocity profile for the free jet was almost uniform when it left the nozzle, but as air was entrained on each side of the jet, the velocity distribution became Gaussian. When the flow attaches to the wall, the boundary layer starts to grow and skews the distribution. A sketch of the distribution is shown in Fig. 1.

The velocity profiles were measured across the channel perpendicular to the flow, (see Fig. 13). For Amplifier No. 1 the channel width was 0.35 inch; for No. 2, 0.30 inch; for No. 3, 0.45 inch. The probe was mounted in a micrometer traverse to give the exact position.

For all three tests the velocity profiles were more Gaussian than skewed so the flow was not well attached to the wall. In each test the flow was first attached to the left wall and pressure readings were taken across the left channel, then the left corona point was turned up until the flow just flipped to the right side where pressure measurements were taken.

In Test 1 the flow was better attached to the right wall than the left, showing that more current was needed to flip from right to left.

The profiles in Test 2 also showed the flow better attached to the right wall.

In Test 3 the profiles on each side were practically idential and they both had a very good Gaussian distribution. The walls could have been longer to give better attachment at higher Reynolds numbers, but this would have added more resistance and the amplifier would have been harder to flip.

The Reynolds numbers for each profile were determined by finding the best operating point of each amplifier since they were different. By comparing the profiles in Tests 1 and 2 it is shown that the flow is better attached on both walls for Amplifier No. 1, at the best operating point of each amplifier.

INTERACTION WIDTH AND CHANNEL ANGLE

By changing the geometry of the flow channel the point of attachment and the stability of the flow can be changed considerably. The first three tests were run to compare the different geometries in each channel and to show how this affected the flow.

It is generally agreed that the channel angle does not influence the flow very much for angles less than 30°, but this did not seem to be true when comparing Tests 1 and 2.[6,7] The current required to flip the flow and hence the control port mass flow needed was greater for the wider-angled Amplifier No. 3. Actually a wider range of channel angles should have been used in testing, and static pressure taps were needed on the channel walls to see if the flow was attached to the wall within one-half the length of the wall from the control port. If the attachment point was too far downstream, the flow would be disrupted by the splitter.

Increasing the interaction width, a, Tests 1 and 3, resulted in a decreased current for flipping. The current should increase when the interaction width has increased from being equal to the nozzle width, d, to twice the nozzle width.[7]

CONTROL PORT AIR FLOW

Test 5 was run to determine the pressure and velocity distributions in the control port for various currents. Three different currents were used, 1.00, 1.25, and 1.50 microamperes. Higher values were tried, but breakdown would occur prematurely when the total pressure probe was inserted in the channel. The static and total pressures were measured every quarter inch form the inlet, (Figs. 47 and 48). The velocity was then calculated (Fig. 50).

With the average velocity at the control port exit, the mass flow needed to flip the flow was calculated, and compared to the mass flow of the jet at various Reynolds numbers.

$$\frac{Q_c}{Q} = \frac{\rho_c A_c V_c}{\rho_n A_n V_n} \qquad (11)$$

Figure 51 shows the mass-flow ratio for Amplifier No. 3. A slight increase in the ratio as the Reynolds number increases indicates that this amplifier operates better at lower flow rates; however, the range of Q_c/Q is considerably better than it is for the large amplifier.

To improve the performance of any size amplifier, the control port must be designed to give the greatest mass flow of air for an optimum current. By using Buckingham's π theorem to solve for the dimensionless groups that describe the flow of air in the control port, a meaningful

comparison of control port geometries can be obtained and the optimum port selected. Appendix III gives a dimensional analysis.

Figure 53 shows the relation between the control port Reynolds number and the corona number. By testing different control ports on the same amplifier and plotting each length ratio curve, the best geometry can be selected since the mass flow of air is directly proportional to the Reynolds number.

IV. CONCLUSIONS AND RECOMMENDATIONS

CONCLUSIONS

Work on the large amplifier was generally unsuccessful. The amplifier was too big and required too much power for operation, but it was conveniently built for test purposes. To find any meaningful information on electric-to-fluidic amplifiers would require a more compact design anyway, so the large amplifier was abandoned.

The small amplifier was successfully miniaturized and proven capable of repeatable operation. The corona wind was still the basic problem with premature breakdown and burnt corona tips caused problems.

The effects of geometric changes on the amplifier operation were generally inconsistent. The two parameters studied were the interaction width, a, and channel angle, α. When a was increased the current required for flipping went down instead of up, and an increase in α caused an increase in current requirements where the effects should have been negligible.

The addition of a plenum chamber to control the flow of air into the control ports does not seem to help the amplifier's performance. A smaller can would be more effective, as evidenced by the test with the hoses directly connected to each other, since the air is blown in one side of the amplifier and sucked out of the other. When the can is too large, it acts just like the room did to the open ports on a smaller scale.

There is a limiting size to an electric-to-fluidic amplifier, but this has not yet been determined. The limit is in the control port where a certain gap must be maintained between the positive and negative electrodes so breakdown does not occur before a sufficient wind is generated. It is noted in this investigation that the limits of the distance, A, are from approximately one-half to one inch for reliable operation.

As Appendix IV shows, the dimension, A, is an important factor in the control-port performance. A more thorough analysis of control-port configurations is needed to make any conclusions about geometry effects.

RECOMMENDATIONS

Any future development on an amplifier should include a detailed study of control port configurations. By designing the amplifier on a still smaller scale and with varying geometries, a good feasibility study could be realized.

A major improvement toward consistency would result by using tungsten wire for the positive point or a suitable substitute to stop erosion during operation. Also, a better machining method to give symmetrical alignment of parts is needed; possibly milling the nozzle, control ports, and flow channel out of a solid piece of Plexiglas. The limitation on accuracy would be the precision in cutting Plexiglas.

APPENDIX I

ANALYSIS OF CORONA DISCHARGE AND THE ANALYTICAL BEHAVIOR OF THE RESULTING CORONA WIND

A corona discharge occurs when a high potential is placed on a sharp point. If the point is positive, free electrons are generated in the gas near the point and move toward the point, gaining very high energy just before reaching the point. During the last few mean free paths, the electrons strike molecules or atoms and create many ions right around the point and cause an avalanche process to begin toward the point. A positive ion space charge results and drifts towards the negative electrode.

If the point is negative, the electrons generated move away from the point and gain a great deal of energy in the high field, but begin to drift slowly as the field weakens, lacking energy to even ionize other particles. The electrons can attach themselves to neutral molecules and form massive negative ions that drift to the anode.

No matter which corona discharge is used, a local mass motion can be produced, measured, and predicted.

To analyze the flow of air through the control nozzle, the following assumptions are made:[1]

(1) The flow is one-dimensional, incompressible, and steady.

(2) The electrical conductivity of a gas, such as air, is very small, approximately zero.

(3) Ions of only one sign exist slightly downstream of the corona wire.

(4) The mobility of the ions was approximately constant.

The current density is

$$J = \sigma_c E + \rho_c v_t \tag{12}$$

where $\sigma_c E$ is taken as 0. v_t is the total velocity of the ions and is equal to the sum of the velocity of the air, v, and the velocity of the ions in the air, v_i. It can be shown that v is very small compared to v_i so that,

$$v_t = v_i \quad . \tag{13}$$

Now

$$v_i = K_o E \; ; \tag{14}$$

so

$$J = \rho_i K_o \cdot E \tag{15}$$

The Navier-Stokes and continuity equations must be satisfied. The Navier-Stokes equation reduces to,

$$F - \frac{\partial p}{\partial x} + \mu \left(\frac{\partial^2 u}{\partial y^2} + \frac{\partial^2 u}{\partial z^2} \right) = 0$$

Now the body force F equals $\rho_i E$, so form Eq. (15)

$$F = J/K_o \tag{16}$$

For a constant cross-sectional, one-dimensional channel,

$$J = I/\text{Area}$$

therefore,

$$F = I/K_o \, (\text{Area}) \tag{17}$$

The Navier-Stokes equation now becomes

$$\frac{I}{K_o} (\text{Area}) - \frac{\partial p}{\partial x} + \mu \left(\frac{\partial^2 u}{\partial y^2} + \frac{\partial^2 u}{\partial z^2} \right) = 0$$

The viscous forces are small compared to body forces for low velocities so the equation is reduced to

$$\frac{I}{K_o} (\text{Area}) = \frac{\partial p}{\partial x}$$

Integrating,

$$p = \frac{I}{K_o} (\text{Area})(x_2 - x_o) \tag{18}$$

where x_o is a reference distance located a short distance from the positive wire.

Equation (18) is Chattock's relation and predicts that the pressure will increase linearly with the current and the distance from the corona wire.

Holding $x_2 - x_0$ constant and introducing a geometric shape factor c, Eq. (18) becomes

$$p = \frac{c}{K_0} I \qquad (19)$$

The pressure drop is calculated at the negative electrode and not the exit of the control port because this analysis only applies to a constant area channel. If the electrodes were mounted at the exit, then for accurate results the corona point would have to be in the narrow region of the port.

The theoretical value of c/K_0 for the control port configuration is 409 psi/amp. For a typical value of $K_0 = 0.216$ in^2/volt-sec at room temperature.[1] A comparison of the theoretical and actual shape factor is shown in Fig. 49.

With the pressure known as a function of the current, the velocity and mass flow from the control port can be calculated and compared with the flow of the main jet.

APPENDIX II

DIMENSIONAL ANALYSIS OF AIR FLOW IN THE CONTROL PORT

From Buckingham's π theorem, with n variables and r basic dimensions, there are (n-r) independent dimensionless groups needed to describe a phenomenon. For the control port air flow, the basic dimensions needed to describe each variable dimensionally are: mass, M; distance, L; time, T; and electric charge, q. To describe the air flow, the following variables and their basic dimensional expressions are needed:

1. Viscosity -μ-	M/LT^2
2. Length -A-	L
3. Control port width at corona point -B-	L
4. Density -ρ-	M/L^3
5. Air velocity -V-	L/T
6. Current -I-	q/T
7. Mobility -K_o-	qT/M

With $n = 7$ and $r = 4$, there are $(7 - 4) = 3$ dimensionless groups needed to express the air flow.

Let V be a function of the other six variables and express them in an infinite series.

$$V = H\,(\mu^a \cdot A^b \cdot B^c \cdot \rho^d \cdot I^f \cdot K_o^g \cdot) + H_2(\mu^a \cdots\cdots)$$

Now express each variable in basic dimensions and use only the first series.

$$\left(\frac{L}{T}\right) = \left(\frac{M}{LT}\right)^a (L)^b\ (L)^c \left(\frac{M}{L3}\right)^d \left(\frac{q}{T}\right)^f \left(\frac{qT}{M}\right)^g$$

The exponents of each basic dimension must be equal by the law of dimensional homogeneity.

$$L: \quad 1 = -a + b + c - 3d$$

$$T: \quad -1 = -a - f + g$$

$$M: \quad 0 = a + d - g$$

$$q: \quad 0 = f + g$$

Solving the four equations for a, c, d, and g in terms of b and f gives,

$$a = 1 - 2f$$
$$c = -1 - b + f$$
$$d = -1 + f$$
$$g = -f$$

Substituting back into the functional relation,

$$V = H\,(\mu)^{1-2f}\,(A)^{b}\,(B)^{-1+f-b}\,(\rho)^{-1+f}\,(I)^{f}\,(K_o)^{-f}$$

Regrouping according to exponents,

$$\frac{\rho VB}{\mu} = H\left[\left(\frac{A}{B}\right), \left(\frac{B\rho I}{\mu^2 K_o}\right)^{f}\right]$$

The left side is recognized as the Reynolds number, the first term on the right is the length ratio, and the other term is denoted as the corona number.

The parameters ρ, ν, and K_o are properties of air and are constants, while A and B are geometric properties of the amplifier and are constant for this test; therefore, the length ratio is constant. The Reynolds number can be plotted against the corona number for a particular value of the length ratio. By testing other control ports, a family of curves can be plotted and the most efficient control port geometry can be determined.

APPENDIX III

DISCUSSION OF CORONA POINT DISTANCE FROM NEGATIVE PLATES

The distance between the corona point and the negative electrodes, denoted by A, is critical in the performance of the control port. With the small amplifier, different positions were used to find the limits of A for efficient operation.

The minimum distance is affected by the amount of voltage that is applied, before breakdown occurs, to create enough current for flipping. Also, the pressure rise is a linear function of the distance from the point and A must be large enough to allow for this pressure rise and hence the velocity for flipping.[3,5] This is shown in Chattock's relation in Appendix I where Δp is a function of current and distance.

The maximum distance is at the point where a large field strength is needed to accelerate the ions, but the voltage supply is not capable of supplying it.

SAMPLE CALCULATIONS

Nozzle Reynolds Number

From Eq. (4)

$$Re = \frac{w}{\mu}\sqrt{2(p_t - p_s)\rho} \qquad (4)$$

$w = 0.20$ inch

$\mu = 11.97 \times 10^{-6}$ $lb_m/ft\text{-}sec$

$\rho = 0.075$ lb_m/ft^3

For $p_t - p_s = 0.10$ inch of water,

$$Re = \frac{0.20}{11.97 \times 10^{-6}}\sqrt{2(0.10)\cdot 0.037(0.075)32.2}$$

$$Re = 2200 \frac{in.}{lb_m/ft\text{-}sec}\left(in.\ H_2O \times \frac{lb_f}{in^2 \cdot in\ H_2O} \times \frac{lb_m}{ft^3} \times \frac{lb_m - ft}{lb_f\text{-}sec^2}\right)^{1/2} =$$

Re = dimensionless

Channel Velocity

From Eq. (6)

$$\frac{V}{V_o} = \sqrt{\frac{P_t - P_s}{P_{to} - P_{so}}} \qquad (6)$$

For Amplifier No. 1, Fig. 9

p_{to} = 0.080 inch of water (gauge)

p_{so} = 0.0 inch of water (gauge)

p_t = 0.064 inch of water (Y = 0.10 inch on left)

p_s = 0.0 inch of water (gauge)

$$\frac{V}{V_o} = \sqrt{\frac{0.064 - 0}{0.080 - 0}} = 0.894$$

Theoretical Shape Factor c/K_o

K_o = 0.216 $in.^2$/volt-sec

Area = 0.25 x 0.40 $in.^2$ = 0.10 $in.^2$

$x_2 - x_o$ = 1.0 inch

$$\frac{c}{K_o} = \frac{x_2 - x_o}{K_o(\text{Area})}$$

$$\frac{c}{K_o} \quad \frac{1.0 \text{ inch} \times 0.736 \text{ ft-lbf/sec-watt} \times 12 \text{ in./ft}}{0.216 \text{ in.}^2\text{/volt-sec} \times 0.10 \text{ in.}^2 \times 1 \frac{\text{amp-volt}}{\text{watt}}}$$

$$\frac{c}{K_o} = 409 \text{ psi/amp}$$

Experimental Shape Factor c/K_o

From Fig. 49

$$\frac{c}{K_o} = \text{slope} = \frac{P_{t2} - P_{t1}}{I_2 - I_1}$$

$$\frac{c}{K_o} = \frac{(12.0 \times 10^{-3} - 7.0 \times 10^{-3})}{(1.50 \times 10^{-6} - 1.00 \times 10^{-6})} \frac{\text{in. } H_2O}{\text{amp}}$$

$$\frac{c}{K_o} = 10^4 \text{ in. } H_2O/\text{amp} \times 0.037 \frac{\text{psi}}{\text{in. } H_2O} = 370 \frac{\text{psi}}{\text{amp}}$$

Mass Flow Ratio

From Eq. (11)

$$Q_c/Q = \frac{\rho_c A_c V_c}{\rho_n A_n V_n}$$

Rewriting Eq. (1),

$$V_n = \left(\frac{\mu}{\rho w}\right) Re$$

$$V_n = \frac{11.97 \text{ Re}}{0.075 \times 0.20 \times 1/12} = 0.962 \times 10^{-2} \left(\frac{\text{ft}}{\text{sec}}\right) Re$$

$$\frac{A_c}{A_n} = \frac{0.15 \text{ in.} \times 0.25 \text{ in.}}{0.20 \text{ in.} \times 0.25 \text{ in.}} = 3/4$$

$$Q_c/Q = 3/4 \frac{V_c \text{ ft/sec}}{0.962 \times 10^{-2} \text{ Re (ft/sec)}}$$

$$Q_c/Q = 78.0 V_c/Re$$

For Amplifier No. 3, the current required for flipping at a Reynolds number of 3370 is 1.00 microampere (Fig. 37). From Fig. 50 for I = 1.00 microampere, V_c = 5.15 ft/sec at the nozzle outlet; therefore

$$\frac{Q_c}{Q} = \frac{78.0 (5.15)}{3370} = 0.12$$

LIST OF EQUIPMENT

1. High Voltage Power Supply
   Type: D. C. Power Supply with built-in filter and transformer
   Rating: 0-30 kV
   Make: Sorensen
   Model: 5030-4

2. D. C. Microammeter
   Type: Px-151
   Rating: 0-15-30-75-150-300 mA
   Make: Westinghouse
   Model: 2913727A17

3. Electrostatic Voltmeter

   Type: Electrostatic double pivoted moving vane
   Rating: 0-10-20-30-40 kV
   Make: Singer Co., Bridgeport, Conn.
   Model: ESH

4. Manometer
   Type: Inclined
   Range: 0-1 inch water
   Make: Ellison Co., Chicago, Ill.

REFERENCES

1. Eiler, Gary P., "An Experimental Investigation of the Influence of Electrostatic Fields on Flow Attachment," A Thesis, Mechanical Engineering Department, The Ohio State University, Columbus, Ohio, 1965.

2. General Electric Company, "Fluid Amplifier State of the Art," Vol. 1, NASA Contractor Report, Contract No. NAS-8-5408, Oct., 1964.

3. Cobine, James Dillon, Gaseous Conductors, Second Edition, Dover Publications, New York, 1960.

4. Loeb, Leonard B., Fundamentals of Electricity and Magnetism, Dover Publications, New York, 1961.

5. Velkoff, Henry R.,"Electrofluidmechanics: A Study of Electrostatic Actions in Fluids," Technical Report No. ASD-TR-61-642, Propulsion Laboratory, Aeronautical Systems Division, Air Force Systems Command, Wright-Patterson Air Force Base, Ohio, Feb., 1962.

6. Comparin, R. A., "On the Limitations and Special Effects in Fluid Jet Amplifiers," ASME Symposium on Fluid Jet Control Devices, Dec., 1962.

7. Comparin, R. A., "Some Effects of Geometry in a Fluid Amplifier," Research Note NZ-4 IBM, Zurich, Switzerland.

8. Bourque, O. and Newman, B. G., "Reattachment of a Two-Dimensional Incompressible Jet to an Adjacent Flat Plate," Aero Quarterly, Vol. 201, August, 1960.

9. Brodin, Gunnar and Nystrom, K. Sture, "Control of a Boundary Layer Fluidistor by Means of Disruptive Discharge," First International Conference on Fluid Logic and Amplification, Sept. 8, 1965.

10. Velkoff, Henry R., "Electrofluidmechanics; Investigation of the Effects of Electrostatic Fields on the Heat Transfer and Boundary Layers," Technical Documentary Report No. ASD-TRD-62-650, Propulsion Laboratory, Aeronautical Systems Division, Air Force Systems Command, Wright-Patterson Air Force Base, Ohio, Sept., 1962.

Unclassified

Security Classification

DOCUMENT CONTROL DATA · R&D

(Security classification of title, body of abstract and indexing annotation must be entered when the overall report is classified)

1. ORIGINATING ACTIVITY (Corporate author) The Ohio State University Research Foundation 1314 Kinnear Road Columbus, Ohio 43212	2a. REPORT SECURITY CLASSIFICATION Unclassified 2b. GROUP

3. REPORT TITLE

A STUDY OF A CORONA WIND DIGITAL FLUID AMPLIFIER ELEMENT

4. DESCRIPTIVE NOTES (Type of report and inclusive dates)

Interim Technical Report

5. AUTHOR(S) (Last name, first name, initial)

Bishop, James L., and Velkoff, Henry R.

6. REPORT DATE	7a. TOTAL NO. OF PAGES	7b. NO. OF REFS
March, 1967	86	10

8a. CONTRACT OR GRANT NO.	9a. ORIGINATOR'S REPORT NUMBER(S)
Da-31-124-ARO-D-246 b. PROJECT NO. 20010501B700 c. 1D12140A142 d.	Technical Report # 3 9b. OTHER REPORT NO(S) (Any other numbers that may be assigned this report)

10. AVAILABILITY/LIMITATION NOTICES

11. SUPPLEMENTARY NOTES	12. SPONSORING MILITARY ACTIVITY
	U. S. Army Research Office - Durham Box CM, Duke Station Durham, North Carolina 27706

13. ABSTRACT

An experimental investigation was conducted on the use of corona wind in air as a means of triggering a fluid "flip-flow" amplifier element. The study centered on the ability to miniaturize the device previously shown possible in other work under the contract. Specific emphasis was also given to the nature of the connecting lines and plenum for the lateral control ports. The results of the investigation indicated that the miniaturized units required very small currents to flip the primary jet, and that the units were very sensitive to the configuration of the plenum and lateral lines.

DD FORM 1 JAN 64 1473

Unclassified

Security Classification

Unclassified
Security Classification

14. KEY WORDS	LINK A		LINK B		LINK C	
	ROLE	WT	ROLE	WT	ROLE	WT
Electrofluidmechanics						
Corona Discharge						
Electric Wind						
Fluid Amplifier						

INSTRUCTIONS

1. **ORIGINATING ACTIVITY:** Enter the name and address of the contractor, subcontractor, grantee, Department of Defense activity or other organization *(corporate author)* issuing the report.

2a. **REPORT SECURITY CLASSIFICATION:** Enter the overall security classification of the report. Indicate whether "Restricted Data" is included. Marking is to be in accordance with appropriate security regulations.

2b. **GROUP:** Automatic downgrading is specified in DoD Directive 5200.10 and Armed Forces Industrial Manual. Enter the group number. Also, when applicable, show that optional markings have been used for Group 3 and Group 4 as authorized.

3. **REPORT TITLE:** Enter the complete report title in all capital letters. Titles in all cases should be unclassified. If a meaningful title cannot be selected without classification, show title classification in all capitals in parenthesis immediately following the title.

4. **DESCRIPTIVE NOTES:** If appropriate, enter the type of report, e.g., interim, progress, summary, annual, or final. Give the inclusive dates when a specific reporting period is covered.

5. **AUTHOR(S):** Enter the name(s) of author(s) as shown on or in the report. Enter last name, first name, middle initial. If military, show rank and branch of service. The name of the principal author is an absolute minimum requirement.

6. **REPORT DATE:** Enter the date of the report as day, month, year, or month, year. If more than one date appears on the report, use date of publication.

7a. **TOTAL NUMBER OF PAGES:** The total page count should follow normal pagination procedures, i.e., enter the number of pages containing information.

7b. **NUMBER OF REFERENCES:** Enter the total number of references cited in the report.

8a. **CONTRACT OR GRANT NUMBER:** If appropriate, enter the applicable number of the contract or grant under which the report was written.

8b, 8c, & 8d. **PROJECT NUMBER:** Enter the appropriate military department identification, such as project number, subproject number, system numbers, task number, etc.

9a. **ORIGINATOR'S REPORT NUMBER(S):** Enter the official report number by which the document will be identified and controlled by the originating activity. This number must be unique to this report.

9b. **OTHER REPORT NUMBER(S):** If the report has been assigned any other report numbers *(either by the originator or by the sponsor)*, also enter this number(s).

10. **AVAILABILITY/LIMITATION NOTICES:** Enter any limitations on further dissemination of the report, other than those imposed by security classification, using standard statements such as:

(1) "Qualified requesters may obtain copies of this report from DDC."

(2) "Foreign announcement and dissemination of this report by DDC is not authorized."

(3) "U. S. Government agencies may obtain copies of this report directly from DDC. Other qualified DDC users shall request through _____."

(4) "U. S. military agencies may obtain copies of this report directly from DDC. Other qualified users shall request through _____."

(5) "All distribution of this report is controlled. Qualified DDC users shall request through _____."

If the report has been furnished to the Office of Technical Services, Department of Commerce, for sale to the public, indicate this fact and enter the price, if known.

11. **SUPPLEMENTARY NOTES:** Use for additional explanatory notes.

12. **SPONSORING MILITARY ACTIVITY:** Enter the name of the departmental project office or laboratory sponsoring *(paying for)* the research and development. Include address.

13. **ABSTRACT:** Enter an abstract giving a brief and factual summary of the document indicative of the report, even though it may also appear elsewhere in the body of the technical report. If additional space is required, a continuation sheet shall be attached.

It is highly desirable that the abstract of classified reports be unclassified. Each paragraph of the abstract shall end with an indication of the military security classification of the information in the paragraph, represented as *(TS), (S), (C), or (U)*.

There is no limitation on the length of the abstract. However, the suggested length is from 150 to 225 words.

14. **KEY WORDS:** Key words are technically meaningful terms or short phrases that characterize a report and may be used as index entries for cataloging the report. Key words must be selected so that no security classification is required. Identifiers, such as equipment model designation, trade name, military project code name, geographic location, may be used as key words but will be followed by an indication of technical context. The assignment of links, rules, and weights is optional.

GPO 886-551